Relationship between the thermopower and entropy of strongly correlated electron systems

V. Zlatić,[1,2] R. Monnier,[3] J. K. Freericks,[4] and K. W. Becker[2]
[1]*Institute of Physics, Bijenička cesta 46, 10001 Zagreb, Croatia*
[2]*Institut für Theoretische Physik, Technische Universität Dresden, 01062 Dresden, Germany*
[3]*ETH Hönggerberg, Laboratorium für Festkörperphysik, 8093 Zürich, Switzerland*
[4]*Georgetown University, Washington, DC 20057, USA*
(Received 14 December 2005; revised manuscript received 18 May 2007; published 20 August 2007)

A number of recent experiments report on a correlation between the low-temperature slope of the thermopower, α/T, and the specific heat coefficient $\gamma=C_V/T$ for heavy fermions and valence fluctuating compounds with Ce, Eu, Yb, and U ions. Assuming that charge and heat currents at low temperatures are transported by quasiparticles, we first derive the universal value for the ratio $q=\alpha/\gamma T$ using macroscopic transport equations. We then calculate the thermal response of the Fermi liquid (FL) regime of the periodic Anderson model and of the Falicov-Kimball model by dynamical mean field theory and find the q ratio. Eventually, we calculate the temperature dependence of $\alpha(T)$ above the FL regime using the "poor man's" approach, which describes the scattering of conduction electrons on the lattice of f ions by the single impurity Anderson model with crystal field (CF) splitting. The overall temperature dependence is obtained by interpolating between the FL and the poor man's solution, and is explained in simple terms. The shape of $\alpha(T)$ is determined by the relative magnitude of the Kondo scale T_K and the CF splitting. Pressure or doping (chemical pressure) affects $\alpha(T)$ by transforming the narrow Kondo resonances into a broad spectral function typical of valence fluctuators. This changes the effective degeneracy of the f state and results in a drastic modification of $\alpha(T)$. Temperature also changes the degeneracy of the f state by populating the excited CF states. Since T_K is strongly pressure dependent, while the CF splitting is not, the shape of $\alpha(T)$ is a sensitive function of pressure or doping. These results explain the near universality of the q ratio and the overall behavior of $\alpha(T)$ in $EuCu_2(Ge_{1-x}Si_x)_2$, $CePt_{1-x}Ni_x$, $YbIn_{1-x}Ag_xCu_4$, and similar systems.

DOI: 10.1103/PhysRevB.76.085122 PACS number(s): 72.15.Jf, 75.30.Mb, 62.50.+p, 75.30.Kz

I. INTRODUCTION

Several recent papers[1–3] reported on a correlation between the low-temperature slope of the thermopower $\alpha(T)/T$ and the specific heat coefficient $\gamma=C_V(T)/T$ for many heavy fermions and valence fluctuating compounds with Ce, Eu, Yb, and U ions. The data show that the ratio $q=\lim_{T\to 0}\alpha/\gamma T$ is about the same, although the absolute values of γ and α/T vary by orders of magnitude.[1–9] At the moment, it is not clear if the deviations from universality arise because of the insufficient accuracy of the data or because the "universal law" is only approximately valid. The difficulty is that neither $\alpha(T)$ nor $C_V(T)$ are linear in the lowest available temperature intervals and an estimate of their zero-temperature slopes is not very accurate. The temperature dependences of $\alpha(T)$ and $C_V(T)$ in various systems might have a different physical origin, and comparing the data on $\alpha(T)/\gamma T$ without a detailed knowledge of the underlying dynamics might lead to erroneous conclusions. Furthermore, the definition of the "zero-temperature limit" can differ considerably for systems with vastly different characteristic temperatures, and at present, it is not clear what the error bars are for the $\alpha/\gamma T$ data. [The $\alpha(T)$ and $C_V(T)$ data are hardly ever available for the same sample.] It would be interesting to test the universality of the q ratio by performing a pressure experiment that transforms Ce- or Eu-based heavy fermion materials into valence fluctuators and Yb-based valence fluctuators into heavy fermion materials. Pressure not only changes the zero-temperature slope by orders of magnitude[10,11] but also has a dramatic effect on the overall temperature dependence of the thermopower, which can be used to infer the low-energy scales of a given system. Although high-pressure experiments are less accurate than ambient pressure ones, the evolution of $\alpha(T)$ or $C_V(T)$ with pressure could be followed and the universality of the q ratio studied in a systematic way. Experiments that provide the low-temperature thermopower and the specific heat on the same sample at various pressures are yet to be performed, but some data are available on the doping dependence (chemical pressure) of $\alpha(T)$ and $C_V(T)$. For example, in $EuCu_2(Ge_{1-x}Si_x)_2$, $CePt_{1-x}Ni_x$ and $YbIn_{1-x}Ag_xCu_4$, doping alters the low-temperature slope of $\alpha(T)$ and $C_V(T)$ by more than 1 order of magnitude[4–9] while barely affecting the q ratio.

A simple relation between α/T and γ is found for a free electron gas and for noninteracting electrons on a lattice in the relaxation time approximation. Under fairly general conditions, one finds the result[12,14] $\alpha(T)\simeq C_V(T)/ne=\mathcal{S}(T)/ne$, where n is the number density of the charge carriers and $\mathcal{S}$ the entropy density. However, noninteracting electrons fail to describe the properties of the compounds mentioned above, and the question arises as to what extent does the "universal relation" between α and $\mathcal{S}$ (or C_V) hold for correlated electrons

On a macroscopic level, an analysis of the charge and heat transport of a thermoelectric in terms of transport equations yields the same relationship between α and $\mathcal{S}$ as the free electron model. This derivation assumes that under isothermal conditions the expectation value of the charge-current density is proportional to the expectation value of the heat current density, which should hold for Fermi liquids (FLs).

On a microscopic level, the q ratio of the periodic Anderson model has been obtained recently by Miyake and Kohno.[13] Using the quasiparticle (QP) approximation, they calculated the Seebeck coefficient from the canonical formula that expresses $\alpha(T)$ as the ratio of two transport integrals.[14] The universal FL behavior is derived by assuming that in addition to the renormalization effects due to the Coulomb interaction between f electrons, the charge and heat transport are affected by the scattering of quasiparticles off residual impurities. This scattering dominates the transport relaxation time and gives rise to a finite residual resistivity ρ_0. In the dilute limit, the impurity concentration drops out of the ratio of the transport integrals and does not appear in the expression for the Seebeck coefficient.

The exact many-body transport coefficients of the periodic spin-1/2 Anderson model have recently been obtained at finite temperatures by Grenzebach *et al.*[15] The electron relaxation is due to the Coulomb repulsion between f electrons, and the model describes heavy fermions and valence fluctuators with small ρ_0. The auxiliary impurity problem generated by the dynamical mean-field theory (DMFT) is solved by the numerical renormalization group (NRG) method, which provides accurate results for the static properties at arbitrary temperature and for the dynamical properties above the FL regime. However, the zero-temperature limit of the transport relaxation time is difficult to obtain by the DMFT+NRG method (due to numerical issues associated with self-consistency), and the validity of the FL laws for the transport coefficients of strongly correlated electrons has not been clearly established.

In this contribution, we discuss the q ratio for the periodic Anderson model and the Falicov-Kimball model, which describe heavy fermions and valence fluctuators with crystal field (CF) split $4f$ states. At $T=0$, the excited CF states are not occupied and we obtain the initial slope of $\alpha(T)$, by the DMFT solution of an effective $\mathcal{L}$-fold degenerate model. The result agrees with that of Miyake and Kohno[13] even though we consider a periodic model with vanishing ρ_0 and have a positive coefficient for the T^2 term of the electrical resistance. We also check that microscopic models with CF splittings properly account for the anomalous features seen in $\alpha(T)$ above the FL regime. At present, the dynamical properties of the Anderson model with CF splitting cannot be obtained by DMFT, and we find the solution using an approximate "poor man's mapping." That is, we assume that the conduction electrons scatter incoherently off the $4f$ ions, relate the transport relaxation time to the single-ion T matrix, and solve the scattering problem by the noncrossing approximation (NCA). The results obtained in such a way[16] show all the typical features observed in heavy fermions and valence fluctuators,[17] and we use them to explain the concentration (chemical pressure) dependence of the q ratio and the evolution of $\alpha(T)$ in $EuCu_2(Ge_{1-x}Si_x)_2$,[3–5] $CePt_{1-x}Ni_x$,[6] and $YbIn_{1-x}Ag_xCu_4$.[8,9,18,19] Our calculations connect the temperature dependence of $\alpha(T)$ at each doping level with the character of the ground state inferred from the initial thermopower slope.

The rest of this contribution is organized as follows. In Sec. II, we introduce the macroscopic transport equations, discuss the Seebeck and Peltier experiments, and find the relationship between the thermopower and the entropy. In Sec. III A, we calculate the Seebeck coefficient of the periodic Anderson model in the FL regime using the DMFT mapping. In Sec. III B, we calculate the finite-temperature behavior using the poor man's mapping. In Sec. III C we discuss the thermoelectric properties of the Falicov-Kimball model using the DMFT approach. In Sec. IV, we use these results to discuss experimental data on the intermetallic compounds mentioned above and present our conclusions in Sec. V.

II. TRANSPORT EQUATIONS

To find the thermoelectric response of correlated systems, we consider the macroscopic charge and energy currents that are given by the statistical averages $\mathbf{J}=\mathrm{Tr}\{\rho_\phi \hat{\mathbf{j}}\}$ and $\mathbf{J}_E^\phi=\mathrm{Tr}\{\rho_\phi \hat{\mathbf{j}}_E^\phi\}$. Here, ρ_ϕ is the density matrix, $\hat{\mathbf{j}}$ the charge-current density, and $\hat{\mathbf{j}}_E^\phi$ the energy current density operators for a system of charged particles in the presence of an external scalar potential ϕ. These operators are obtained by commuting the Hamiltonian with the charge and energy polarization operators;[14] the current densities obtained in such a way provide the macroscopic currents that satisfy the appropriate continuity equations.[20] Assuming that the external potential couples to the charge density, a direct calculation shows[21] that $\hat{\mathbf{j}}$ is field independent and $\hat{\mathbf{j}}_E^\phi=\hat{\mathbf{j}}_E+\phi\hat{\mathbf{j}}$, where $\hat{\mathbf{j}}_E$ is the energy current density defined by the field-free Hamiltonian. The macroscopic energy current $\mathbf{J}_E=\mathrm{Tr}\{\rho_\phi \hat{\mathbf{j}}_E\}$ does not satisfy the continuity equation in the presence of the external potential but is easily determined by a gradient expansion of ρ_ϕ. This yields linearized equations $\mathbf{J}=L_{11}\mathbf{x}_c+L_{12}\mathbf{x}_E$ and $\mathbf{J}_E=\mathbf{J}_{E_\phi}-\phi\mathbf{J}=L_{21}\mathbf{x}_c+L_{22}\mathbf{x}_E$, where $\mathbf{x}_c=-\nabla\phi-T\nabla(\mu/eT)$ and $\mathbf{x}_E=-\nabla T/T$ are the generalized forces, μ is the chemical potential, and $e=-|e|$ is the electron charge. The (linear-response) expansion coefficients are given by the correlation functions

$$L_{ij}^{\alpha\beta}=\lim_{s\to 0}\frac{1}{V}\int_0^\infty dt e^{-st}\int_0^\beta d\beta\langle\hat{\mathbf{j}}_i^\alpha(-t-i\beta)\hat{\mathbf{j}}_j^\beta(0)\rangle_0, \quad (1)$$

where $\langle\hat{\mathbf{j}}_i^\alpha\hat{\mathbf{j}}_j^\beta\rangle_0=\mathrm{Tr}\{\rho\hat{\mathbf{j}}_i^\alpha\hat{\mathbf{j}}_j^\beta\}$ denotes the statistical average in the absence of the external potential and $\hat{\mathbf{j}}_1^\alpha$ and $\hat{\mathbf{j}}_2^\beta$ denote the $q=0$ Fourier components of $\hat{\mathbf{j}}^\alpha(x)$ and $\hat{\mathbf{j}}_E^\beta(x)$, respectively ($\alpha$ and β denote the coordinate axes). In what follows, we assume a homogenous and isotropic conductor in the absence of a magnetic field and consider only a single Cartesian component of $\hat{\mathbf{j}}$ and $\hat{\mathbf{j}}_E$ (this is appropriate for cubic systems).

Thermoelectric effects are usually described in terms of the heat current rather than the energy current. Hence, we transform $\mathbf{J}$ and $\mathbf{J}_E$ to $\mathbf{J}$ and $\mathbf{J}_Q=\mathbf{J}_E-(\mu/e)\mathbf{J}$ to yield[12,14]

$$\mathbf{J}=-\sigma\nabla\phi-\sigma\alpha\nabla T, \quad (2)$$

$$\mathbf{J}_Q=\alpha T\mathbf{J}-\kappa\nabla T, \quad (3)$$

where $\sigma=L_{11}$, $\alpha T=(L_{12}/L_{11}-\mu/e)$, and $\kappa T=(L_{22}-L_{12}^2/L_{11})$. A simple analysis shows that $\sigma(T)$, $\alpha(T)$, and $\kappa(T)$ are the

isothermal electrical conductivity, the Seebeck coefficient and the thermal conductivity, respectively.[12,22] The Onsager relation[12] gives $\alpha T=\Pi$, where Π is the Peltier coefficient.

The stationary temperature distribution across the sample is obtained from the total energy current in a field $\mathbf{J}_E^{\phi}=\mathbf{J}_Q+(\phi+\mu/e)\mathbf{J}$, which satisfies the energy continuity equation[20] $\dot{E}_{\phi}=-\mathrm{div}\,\mathbf{J}_E^{\phi}=0$ and leads to the Domenicali equation[22]

$$\dot{E}_{\phi}=\mathrm{div}(\kappa\nabla T)+\frac{\mathbf{J}^2}{\sigma}-T\mathbf{J}\cdot\nabla\alpha=0. \tag{4}$$

The solution of Eqs. (2)–(4), with appropriate boundary conditions, completely specifies the thermoelectric response of the system. In principle, the above procedure could be used to connect the theoretical model of a given material with the phenomenological transport coefficients and should explain the experimentally established relationship between $\alpha(T)/T$ and γ. However, for general many-body systems, such a program cannot be completed and, at first sight, it is not obvious that the transport coefficients, which depend on the dynamical properties of the system, are simply related to the thermodynamic quantities, which depend only on the static properties. On a macroscopic level, the relationship between α and $\mathcal{S}$ is obtained by solving Eqs. (2) and (3) once with the boundary conditions corresponding to the measurement of the Seebeck coefficient and once with those appropriate for the measurement of the Peltier coefficient. The main advantage of such a simple derivation is that it clearly indicates the terms that are being neglected.

In the Seebeck setup (an open circuit without net charge current), the thermoelectric voltage is induced by the heat flow due to the temperature gradient. The Seebeck voltage appears because the charged particles diffuse from the hot to the cold end, and the imbalance of charge gives rise to a potential gradient across the sample. In a stationary state, a quasiparticle picture says that the electrical energy required to transfer n electrons from the hot end to the cold end against the voltage ΔV is balanced by the change in thermal energy (that is, the heat). Neglecting the shift of the quantum states due to the external potential, we approximate $ne\Delta V\simeq\mathcal{S}_n\Delta T$, where n is the particle density and $\mathcal{S}_n$ the entropy density of the charge carriers. The Seebeck coefficient is obtained from the ratio $\Delta V/\Delta T$, where $\Delta V=-\int_0^a dx\nabla\phi(\mathbf{x})$ is the voltage change and $\Delta T=\int_0^a dx\nabla T(\mathbf{x})$ the temperature drop between the end points of a sample of length a. For constant $\alpha(x)$, Eq. (2) gives $\Delta V=\alpha\Delta T$, and we find the approximate relationship between the Seebeck coefficient and the entropy,

$$\alpha(T)=\frac{\mathcal{S}_n(T)}{en}. \tag{5}$$

In the Peltier setup, a constant electrical current passing through a junction of two different thermoelectrics gives rise to an additional heat current emanating at the junction. In a stationary state, the normal component of currents and temperature are continuous across the junction, but ∇T and the transport coefficients are discontinuous. Using Eq. (3), we find at the interface $\kappa_s\nabla T|_s-\kappa_l\nabla T|_l=\mathbf{J}T(\alpha_s-\alpha_l)$, where s and l denote the "sample" and "leads," respectively. Thus, the heat brought to and taken from the junction by the thermal conductivity differs by $\Pi_{sl}\mathbf{J}=(\Pi_s-\Pi_l)\mathbf{J}$, where Π_{sl} is the relative and Π_l and Π_s the absolute Peltier coefficients of the two materials, $\Pi_{s,l}=T\alpha_{s,l}(T)$. The junction generates an additional heat current $\Pi_{sl}\mathbf{J}$, which maintains the stationary state by absorbing (or releasing) heat from the environment. The Peltier heat appears because the excitation spectra on the two sides of the interface are different, so that the charge transfer produces a reversible entropy change. (The entropy of n particles is determined by the structure of the energy levels over which the current carriers are distributed.)

Under stationary isothermal conditions, and for currents flowing in the x direction, we have $\alpha(T)=J_Q/TJ$, where J_Q is the Peltier heat current. Assuming that the stationary state is maintained by a heat source at one end and a heat sink at the other end of the sample and that the charge and heat flow is uniform, with a drift velocity $\mathbf{v}$, we can write $\mathbf{J}=ne\mathbf{v}$ and $\mathbf{J}_Q=Q_n\mathbf{v}$. Here, $Q_n=\alpha Tne$ is the Peltier heat generated at the lead-sample interface and transported by the current in the lead to the sink. Defining the reversible thermoelectric entropy density as $\mathcal{S}_n(T)=Q_n/T$ again gives Eq. (5). Finally, multiplying both sides of Eq. (5) by N_Ae, where N_A is Avogadro's constant, and dividing by the molar entropy $\mathcal{S}_N(T)=\mathcal{S}_n(T)\Omega$, where Ω is the molar volume of the material under study, we obtain a dimensionless parameter,

$$q=N_A\frac{e\alpha(T)}{\mathcal{S}_N(T)}=\left(\frac{N}{N_A}\right)^{-1}, \tag{6}$$

which characterizes the thermoelectric material in terms of an effective charge carrier concentration per f.u. (or the Fermi volume V_F of the charge carriers). For Fermi liquids, $\mathcal{S}(T)=\gamma T$ at low temperatures, such that

$$q=N_Ae\frac{\alpha(T)}{\gamma T}, \tag{7}$$

which is used by Behnia *et al.*[2] Throughout this paper, α is expressed in μV/K and C_V and $\mathcal{S}$ in J/(K mol), and the Faraday number is $N_Ae=9.6\times10^4$ C/mol.

We now comment on the validity of the above approximations. As mentioned already, the entropy of the charge carriers in the steady state, which characterizes the Seebeck setup, is not the same as the equilibrium entropy because the steady-state potential is different at the hot and the cold end. As regards the Peltier setup, the average values of the current density operators are not simply proportional to the particle density, and the definition used in Eq. (6) neglects all the operator products that lead to higher-order powers in the particle density. This amounts to describing the low-energy excitations of the system by quasiparticles and approximating the many-body interactions by self-consistent fields.

Furthermore, we should take into account that the entropy $\mathcal{S}_n$ in Eq. (5) or $\mathcal{S}_N$ in Eq. (6) is not the full entropy $\mathcal{S}$ of the system but only the entropy of the charge carriers appearing in the transport equations. For example, the total entropy $\mathcal{S}$ might have contributions S_M coming from additional degrees of freedom, such as localized paramagnetic states, magnons, and phonons, which do not participate in the charge transport and are only weakly coupled to the charge carrying modes. Assuming $\mathcal{S}=\mathcal{S}_N+\mathcal{S}_M$ but neglecting the contribution of

these additional degrees of freedom to the charge transport, we get the experimentally determined quantity

$$\tilde{q} = N_A \frac{e\alpha(T)}{\mathcal{S}(T)} = \frac{N_A}{N} \frac{1}{1 + \mathcal{S}_M(T)/\mathcal{S}_N(T)}, \tag{8}$$

which could be much reduced with respect to $q=N_A/N$ given by Eq. (6). The experimental values $\tilde{q}$ depend not only on the concentration of carriers but also on temperature, and to get the universal ratio one might need a very low temperature, where $\mathcal{S}_M \ll \mathcal{S}_N$. This behavior is similar to deviations of the Wiedemann-Franz law from the ideal metallic behavior whenever the phonon contribution to the heat current is substantial—in order for the Wiedemann-Franz law to hold, the phonon contribution to the thermal conductivity has to be much smaller than the electronic contribution.

The Seebeck coefficient appearing in Eqs. (5)–(8) should also be treated with care. If there are several conductivity channels, the total thermopower is a weighted sum of all the components $\sigma\alpha=\Sigma_j\sigma_j\alpha_j$, where $\sigma=\Sigma_j\sigma_j$, and there might be some cancellations in the thermopower sum. But $\mathcal{S}$ has different vertex corrections, and the specific heat is not affected by these cancellations. Similarly, if there are several scattering channels for conduction electrons, vertex corrections give rise to interferences that affect the thermopower (like in the Friedel phase shift formula[23]). Even if we neglect interference effects and use the Nordheim-Gorter rule[24] ($\rho\alpha=\Sigma_j\rho_j\alpha_j$, where $\rho=\Sigma_j\rho_j$ and ρ_j and α_j are the resistivity and thermopower due to the jth scattering channel), the α_j terms in the weighted sum might have different signs and cancel. Thus, unless one of the channels dominates, $\tilde{q}$ is nonuniversal and temperature dependent, and the interpretation becomes difficult. We also remark that the heat conductivity of magnons and phonons can give rise to phonon-drag and spin-drag contributions to $\alpha(T)$, which are not included in Eq. (6) or (8). However, at low temperatures, those contributions are expected to be small.

III. MODEL CALCULATION OF THE SEEBECK COEFFICIENT

Considering the limitations and uncertainties mentioned above, it is somewhat surprising that in many correlated systems the low-temperature ratio of the thermopower and the specific heat comes quite close to the universal value given by Eq. (7). In what follows, we show that the universal law of Sakurai[1] and Behnia *et al.*[2] holds for the periodic Anderson model with on-site hybridization and for the Falicov-Kimball model. We also show that these models of strongly correlated electrons explain the full temperature dependence of the Seebeck coefficient observed in the intermetallic compounds with Ce, Eu, and Yb ions. The charge-current operator in both models is

$$\hat{\mathbf{j}} = e\sum_{\mathbf{k}\sigma} \mathbf{v}_{\mathbf{k}} c^{\dagger}_{\mathbf{k}\sigma} c_{\mathbf{k}\sigma}, \tag{9}$$

where σ labels the symmetry channels [irreducible representations to which the (conduction) c electrons belong] and $\mathbf{v}_{\mathbf{k}}=\nabla\epsilon(\mathbf{k})$ is the velocity of the unperturbed c electrons. Calculating the heat current density operators for a constant hybridization in $\mathbf{k}$ space, we verify explicitly the Jonson-Mahan theorem[25] and find for each symmetry channel the static conductivity

$$\sigma(T) = \int d\omega \left(-\frac{df}{d\omega}\right) \Lambda(\omega, T) \tag{10}$$

and the thermopower

$$\alpha(T) = -\frac{1}{|e|T} \frac{\int d\omega \left(-\frac{df}{d\omega}\right) \omega\Lambda(\omega, T)}{\int d\omega \left(-\frac{df}{d\omega}\right) \Lambda(\omega, T)}. \tag{11}$$

The excitation energy ω is measured with respect to μ, $f(\omega)=1/[1+\exp(\beta\omega)]$ is the Fermi-Dirac distribution function, and $\Lambda(\omega,T)$ is the charge-current–charge-current correlation function[14] (our result differs from Mahan's by an additional factor of e^2 from the charge-current operators). In the low-temperature FL limit, the charge-current–charge-current correlation function is approximately found from the reducible vertex function by

$$\Lambda(\omega, T) = \frac{e^2}{V}\sum_{\mathbf{k}\sigma} \mathbf{v}_{\mathbf{k}}^2 G_c^{\sigma}(\mathbf{k}, \omega + i\delta) G_c^{\sigma}(\mathbf{k}, \omega - i\delta) \times \gamma^{\sigma}(\mathbf{k}, \omega + i\delta, \omega - i\delta). \tag{12}$$

Here, $G_c^{\sigma}(\mathbf{k}, \omega \pm i\delta)$ are the momentum and energy-dependent retarded and advanced Green's functions of the conduction electrons and $\gamma^{\sigma}(\mathbf{k}, \omega+i\delta, \omega-i\delta)$ is the analytic continuation from the imaginary axis into the complex plane of the (reducible) scalar vertex function $\gamma^{\sigma}(\mathbf{k}, i\omega_n)$, which is defined by the diagrammatic expansion of the current-current correlation function.[14] The calculations are model dependent, and, in what follows, we consider separately the periodic Anderson model and the Falicov-Kimball model.

One can also determine the current-current correlation function exactly within DMFT,[26] where the vertex corrections vanish, and

$$\Lambda(\omega, T) = \frac{e^2}{V}\sum_{\mathbf{k}\sigma} \mathbf{v}_{\mathbf{k}}^2 [\mathrm{Im}\, G_c^{\sigma}(\mathbf{k}, \omega + i\delta)]^2. \tag{13}$$

This form is useful if $G_c^{\sigma}(\mathbf{k}, \omega+i\delta)$ is known for all $\mathbf{k}$ and ω points; we use it for the Falicov-Kimball model[27,28] since the latter does not have FL behavior in general.

A. Periodic Anderson model: The low-temperature DMFT solution

The periodic Anderson model is defined by the Hamiltonian

$$H_A = H_c + H_f + H_{cf}, \tag{14}$$

where H_c describes the c electrons hopping on the lattice, H_f describes the $4f$ states localized at each lattice site, and H_{cf} describes the c-f hybridization. The c and f electrons have $\mathcal{L}$ internal degrees of freedom (channels), and we consider the

model with an infinitely strong Coulomb repulsion between f electrons (or f holes), which does not allow two f electrons to occupy the same lattice site. The total number of c and f electrons per site is n_c and n_f, respectively. We strictly enforce the constraint $n_f \leqslant 1$ (or $n_f^h \leqslant 1$), at each lattice site choose $n_c \leqslant 1$, and conserve the total number of electrons $n = n_c + n_f$ by adjusting a common chemical potential μ. The unrenormalized density of states (DOS) of c electrons in each channel is $\mathcal{N}_c^0(\epsilon) = \Sigma_{\mathbf{k}} \delta(\epsilon - \epsilon_{\mathbf{k}})$, where $\epsilon_{\mathbf{k}}$ is the conduction-electron dispersion. We assume $\mathcal{N}_c^0(\epsilon)$ to be a symmetric, slowly varying function of half-width D, which is the same in all channels, and measure all the energies, except ω, with respect to its center. In the case of heavy fermions and valence fluctuators with Ce ions, the magnetic state is represented by CF levels, occupied by a single f electron. We consider $M-1$ excited CF levels separated from the CF ground state at E_f^0 by energies $\Delta_i \ll |E_f^0|$, where $i = 1, \ldots, M-1$. Each CF state belongs to a given irreducible representation of the point group Γ_i. The spectral functions of the unrenormalized f states are given by a set of delta functions at E_f^0 and $E_f^i = E_f^0 + \Delta_i$. The degeneracy is $\mathcal{L}_i$ and $\mathcal{L} = \Sigma_i \mathcal{L}_i$. The mixing matrix element V_i connects the c and f states belonging to the same irreducible representation and, for simplicity, we take $V_i = V$ for all channels; i.e., the hybridization is characterized by the parameter $\Gamma = \pi V^2 \mathcal{N}_c^0(0)$. The properties of the model depend in an essential way on the CF splitting and the effective c-f coupling constant $g = \Gamma / \pi |E_f - \mu|$, where $E_f = \Sigma_i \mathcal{L}_i E_f^i / \mathcal{L}$. For $\mathcal{L} > 2$ and strong correlation between the f electrons, the condition $n_f \leqslant 1$ makes the model extremely asymmetric. The limit $n_f \simeq 1$ can only be reached for $g \to 0$. An application of pressure or chemical pressure (doping) to Ce systems is modeled by an increase of the bare coupling g. The increase in g gives rise to a monotonic reduction of n_f and makes the Ce ions less magnetic. In the case of europium, the nonmagnetic $4f^6$ state is a Hund's singlet and the magnetic state is a degenerate ($4f^7$) Hund's octet with a full rotational invariance. The Eu ion fluctuates between the two configurations by exchanging a single electron with the c band, and we model the pressure effects in the same way as for Ce. In the case of ytterbium, the nonmagnetic state is the full-shell $4f^{14}$ configuration and the magnetic one is the $4f^{13}$ configuration, which can be split by the CF. Here, pressure or chemical pressure reduces g and enhances the number of f holes, which makes the Yb ions more magnetic.

We consider first the low-temperature solution that takes into account the coherent scattering on the f lattice. At low temperature, the excited CF states are unoccupied and the calculations can be performed for an effective spin-degenerate model, where the effective degeneracy is set by the CF ground state. The correlations are treated by the DMFT, which is exact in the limit of infinite dimensions.[29–31] To simplify the notation, we drop the spin label in this section. Using the equations of motion for the imaginary time Green's functions, making the Fourier transform to Matsubara frequencies, and analytically continuing into the complex energy plane, we obtain the Dyson equations for the c- and f-electron Green's functions,

$$G_c(\mathbf{k}, z) = \frac{z - (E_f - \mu) - \Sigma_f(\mathbf{k}, z)}{[z - (\epsilon_{\mathbf{k}} - \mu)][z - (E_f - \mu) - \Sigma_f(\mathbf{k}, z)] - V^2} \tag{15}$$

and

$$G_f(\mathbf{k}, z) = \frac{z - (\epsilon_{\mathbf{k}} - \mu)}{[z - (\epsilon_{\mathbf{k}} - \mu)][z - (E_f - \mu) - \Sigma_f(\mathbf{k}, z)] - V^2}, \tag{16}$$

where $\Sigma_f(\mathbf{k}, z)$ is the f-electron self-energy (the self-energy and Green's functions are identical for each of the $\mathcal{L}$ different f states). The retarded (advanced) Green's functions are defined for z in the upper (lower) part of the complex plane and on the real axis for $\omega^{\pm} = \lim_{\delta \to 0} (\omega \pm i\delta)$. The self-energy of the c electrons is

$$\Sigma_c(\mathbf{k}, z) = \frac{V^2}{z - (E_f - \mu) - \Sigma_f(\mathbf{k}, z)}. \tag{17}$$

The DMFT self-energies are $\mathbf{k}$ independent, $\Sigma_f(\mathbf{k}, z) = \Sigma_f(z)$ and $\Sigma_c(\mathbf{k}, z) = \Sigma_c(z)$, which allows us to find the solution by mapping the local Green's function, $\Sigma_{\mathbf{k}} G_f(\mathbf{k}, z)$, onto the Green's function of an auxiliary single impurity Anderson model,

$$G_f(z) = \frac{1}{z - (E_f - \mu) - \Delta(z) - \Sigma_f(z)}, \tag{18}$$

where the bath function $\Delta(z)$ is obtained from the self-consistent solution of Eqs. (15)–(18). This model describes a single f electron distributed over $\mathcal{L}$-fold degenerate spin states coupled to a bath. The irreducible self-energy of the lattice and the impurity are given by the same functional, $\Sigma_f[\Sigma_{\mathbf{k}} G_f(\mathbf{k}, \omega)] = \Sigma_f[G_f(\omega)]$. The self-consistency requires that the impurity spectral function, $A(\omega) = -\mathrm{Im}\, G_f(\omega^+)/\pi$, coincides with the local f-DOS of the lattice, $\mathcal{N}_f(\omega) = \Sigma_{\mathbf{k}} A_f(\mathbf{k}, \omega)$, where

$$A_f(\mathbf{k}, \omega) = -\frac{1}{\pi} \mathrm{Im}\, G_f(\mathbf{k}, \omega^+). \tag{19}$$

Since n_f is the same on the impurity and the lattice, the impurity model is highly asymmetric. In what follows, we consider the DMFT solution in the FL regime.

For $\omega \simeq 0$, we assume that the ω dependence of $\Delta(\omega)$ is much slower than that of $\mathrm{Im}\, \Sigma_f(\omega^+, T)$ and that $\Delta(\omega) \simeq \Delta(0) = i\Delta_0$. The positive definiteness of $\mathcal{N}_f(\omega)$ requires $\Delta_0 < 0$ and from the causality of the problem, it follows that $\mathrm{Im}\, \Sigma_f(\omega^+, T)$ is negative on the real ω axis. At $T = 0$, the imaginary part of $\Sigma_f(\omega^+, T)$ has a maximum at $\omega = 0$, such that[32] $\mathrm{Im}\, \Sigma_f(0) = 0$, $\mathrm{Im}[\partial \Sigma_f / \partial \omega]_{\omega = 0^+} = 0$, and $\mathrm{Im}[\partial^2 \Sigma_f / \partial \omega^2]_{\omega = 0^+} < 0$. In the limit $\omega^+ \to 0$, a linear expansion of $\tilde{\epsilon}_f(\omega) = E_f + \mathrm{Re}\, \Sigma_f(\omega^+)$ gives $\omega - [\tilde{\epsilon}_f(\omega) - \mu] \simeq (\omega - \tilde{\omega}_f) Z_f^{-1}$, where $\tilde{\omega}_f = [\tilde{\epsilon}_f(0) - \mu] Z_f$ is the renormalized position of the f level and $Z_f^{-1} = (1 - \partial \Sigma_f / \partial \omega)_{\tilde{\omega} = 0}$ the renormalization factor.

The charge-current correlation function for the FL at low temperature follows from the identity $G_c(\mathbf{k}, \omega^+) G_c(\mathbf{k}, \omega^-) = -A_c(\mathbf{k}, \omega) / \mathrm{Im}\, \Sigma_c(\omega^+, T)$, where

$$A_c(\mathbf{k},\omega) = -\frac{1}{\pi}\,\mathrm{Im}\,G_c(\mathbf{k},\omega^+) \tag{20}$$

is the spectral function of c electrons. We calculate $\Lambda(\omega,T)$ using Eq. (12) instead of Eq. (13) since it is the dominant contribution when $T\to 0$. This gives

$$\Lambda(\omega,T) = \frac{\tau(\omega,T)}{V}\sum_{\mathbf{k}} e^2 {v_{\mathbf{k}}}^2 A_c(\mathbf{k},\omega), \tag{21}$$

where $\tau(\omega,T)$ denotes the transport relaxation time

$$\tau(\omega,T) = \frac{1}{-\,\mathrm{Im}\,\Sigma_c(\omega^+,T)}. \tag{22}$$

Since the factor $(-df/d\omega)$ restricts the transport integrals to the Fermi window, $|\omega| \leqslant k_B T$, the main contribution to the transport coefficients is due to the $\mathbf{k}$ points in the vicinity of the renormalized Fermi surface (FS), which is defined by the equation $(\epsilon_{\mathbf{k}}-\mu)[\tilde{\epsilon}_f(0)-\mu]=V^2$. In this narrow region of $(\mathbf{k},\omega)$ space, we approximate $v_{\mathbf{k}}^2$ by its FS average, $\langle v_{k_F}^2\rangle$ and find the usual result,

$$\Lambda(\omega,T) = e^2\langle {v_{k_F}}^2\rangle \mathcal{N}_c(\omega)\tau(\omega,T), \tag{23}$$

where the renormalized c-DOS is defined by

$$\mathcal{N}_c(\omega) = \sum_{\mathbf{k}} A_c(\epsilon_{\mathbf{k}},\omega). \tag{24}$$

The approximate FL charge-current correlation function, given by Eq. (23), coincides with the exact DMFT result[27,28] only in the limit $T,\omega\to 0$ (the exact result has another term, which can be neglected as $T\to 0$ but is important at finite T or for non-FL systems).

The renormalized low-energy densities of states are calculated by the Fermi liquid theory of Yamada and Yosida[33] and Yamada,[34] which approximates the spectral functions by their singular parts. Using the fact that $A_c(\epsilon_{\mathbf{k}},\omega)$ and $A_f(\epsilon_{\mathbf{k}},\omega)$ depend on $\mathbf{k}$ only through $\epsilon_{\mathbf{k}}$ [see Eqs. (15) and (16) and recall that Σ_f is independent of $\mathbf{k}$ in DMFT], we can write in each symmetry channel

$$\mathcal{N}_f(\omega) = \int d\epsilon \mathcal{N}_c^0(\epsilon) A_f(\epsilon,\omega) \tag{25}$$

and

$$\mathcal{N}_c(\omega) = \int d\epsilon \mathcal{N}_c^0(\epsilon) A_c(\epsilon,\omega), \tag{26}$$

where $\mathcal{N}_c^0(\epsilon)$ is the unrenormalized density of states of the c electrons. The full DOS is obtained by multiplying the above expressions by $\mathcal{L}$. Close to the renormalized FS, the main contribution to $\mathcal{N}_f(\omega)$ and $\mathcal{N}_c(\omega)$ comes from the singular parts of the spectral functions (once again, for the FL at low T). Estimating the average Fermi momentum of the hybridized states by the Luttinger theorem and keeping just the singular parts of the integrands give the zero-temperature results[35,36]

$$\mathcal{N}_c(\omega) = \mathcal{N}_c^0\left(\omega+\mu-\frac{V^2}{\omega-\tilde{\epsilon}_f(\omega)+\mu}\right), \tag{27}$$

from which we find

$$\mathcal{N}_f(0) = \pm\frac{n_c}{\mathcal{L}}\frac{Z_f}{\tilde{\omega}_f}. \tag{28}$$

The upper sign applies to Ce and Eu compounds, in which the renormalized f level is above μ ($\tilde{\omega}_f>0$) and the lower to Yb compounds in which $\tilde{\omega}_f<0$. Introducing the specific heat coefficient of the periodic Anderson model, $\gamma \simeq (\pi^2 k_B^2/3)\mathcal{L}\mathcal{N}_f(0)Z_f^{-1}$, we find from Eq. (28) the relationship $\tilde{\omega}_f=(\pi^2 k_B^2/3)(n_c/\gamma)$.

It is a challenge to determine the low-temperature transport relaxation time given in Eq. (22) because the right-hand side diverges when ω and T both equal zero. However, using $\mathrm{Im}\,\Sigma_f(\omega^+,T)\approx -|c|(\omega^2+\pi^2T^2/2)$, which holds for a FL in the limit of strong correlations,[33,34] we see that the proper way to take the limit of $T\to 0$ is to first consider the limit $\omega\to 0$ at finite T and then examine what happens as $T\to 0$. Doing so will allow for a proper calculation of the Seebeck coefficient, which is finite, even though it is determined as the ratio of two integrals, each becoming infinite as $T\to 0$. With these ideas in mind, we substitute $\Sigma_c(\omega^+,T)$ given by Eq. (17) in Eq. (22) and obtain $\tau(\omega,T)$, taking the limit in such a way that $\omega\to 0$ before $\delta\to 0$. At low temperature, we do not expect $-\tilde{\epsilon}_f(\omega,T)+\mu$ to vanish because it vanishes for the single-band model at half filling, and we have a multiband model far from half filling. In the following, we assume that $-\tilde{\epsilon}_f(\omega,T)+\mu$ is much larger (in absolute magnitude) than ω or T in the low-frequency and low-temperature regime. For a given value of V, E_f, and n, we calculate $\Sigma_f(\omega)$, $\tilde{\epsilon}_f(\omega,T)$, $\mathcal{N}_f(\omega)$, $\mathcal{N}_c(\omega)$, n_f, and n_c by the DMFT procedure, find μ from the condition $n_f+n_c=n$, and obtain $\tau(\omega,T)$.

The low-temperature Seebeck coefficient follows from the Sommerfeld expansion of Eqs. (11) and (23). It is a weighted sum of the contribution of all the symmetry channels, which, all of them being equivalent, is equal to the single channel value. To lowest order,

$$\frac{\alpha(T)}{T} = -\frac{\pi^2}{3}\frac{k_B^2}{|e|}\left[\frac{1}{\mathcal{N}_c(\omega)}\frac{\partial\mathcal{N}_c(\omega)}{\partial\omega}+\frac{1}{\tau(\omega)}\frac{\partial\tau(\omega)}{\partial\omega}\right]_{\omega,T=0}. \tag{29}$$

The quantity $\lim_{T\to 0}\tau_0(T)=\lim_{T\to 0}[\lim_{\omega\to 0}\tau(\omega,T)]$ diverges, but the expressions given by the ratio of two transport integrals, such as the one in Eq. (11) or the logarithmic derivative in Eq. (29), remain finite at $T=0$. Using $\mathrm{Im}\,\Sigma_f(\omega)\simeq\omega^2$ at $T=0$, we obtain from Eqs. (17), (22), and (28) the zero-temperature result,

$$\frac{d}{d\omega}[\ln\tau(\omega)]\bigg|_{\omega=0} \simeq \mp\frac{2\mathcal{L}\mathcal{N}_f(0)Z_f^{-1}}{n_c}. \tag{30}$$

From Eq. (27), we find for a slowly varying $\mathcal{N}_0(\omega)$ that $(d/d\omega)[\ln\mathcal{N}_c(\omega)]_{\omega=0} \ll (d/d\omega)[\ln\tau(\omega)]_{\omega=0}$ and, neglecting the first term in Eq. (29), obtain the FL law,

$$\alpha(T) = \pm \frac{2\gamma T}{|e|n_c} = \frac{2\gamma T}{|e|n_c} \frac{\tilde{\omega}_f}{|\tilde{\omega}_f|}. \tag{31}$$

The initial slope of the low-temperature Seebeck coefficient is positive when the Kondo resonance is above μ, which corresponds to the intermetallic compounds with Ce and Eu ions. It is negative when the Kondo resonance is below μ, which corresponds to the intermetallics with Yb ions.

The above considerations apply to systems that fluctuate between a nonmagnetic and an $\mathcal{L}$-fold degenerate magnetic state, such as heavy fermions with a large Kondo scale and valence fluctuators. They should also apply to heavy fermions with CF splittings because at low enough temperatures the excited CF states are unoccupied and the magnetic configuration is characterized by the lowest CF state. Using Eq. (31) and the charge neutrality condition $n=n_f+n_c$, we find that the reduction of n_f by pressure or chemical pressure slightly reduces the q ratio.

Note that we calculate the transport properties of strongly correlated systems following a completely different route than Miyake and Kohno,[13] even though the QP dispersion obtained from the secular equation $(\omega-\epsilon_{\mathbf{k}}+\mu)[\omega-\tilde{\epsilon}_f(\omega)-\mu]=V^2$ is exactly the same. In Ref. 13, the QP bands are obtained for an effective model of hybridized fermions with renormalized parameters that take into account the on-site correlation. However, doubly occupied f states are not explicitly excluded from the Hilbert space of the effective Hamiltonian, and the number of f electrons is restricted to $n_f \leqslant 1$ only on average. In such a fermionic model, the charge and heat current density operators in the QP representation are given by quadratic forms that commute with the effective Hamiltonian. The Jonson-Mahan theorem applies, and the low-temperature thermopower is obtained from the canonical expression in Eq. (29). The quasiparticle relaxation is due to scattering off external impurities, which give rise to a finite residual resistivity, and the logarithmic derivatives of the QP density of states and the transport relaxation time are of the same order of magnitude.

In our approach, we assume an infinitely large Coulomb interaction and use QP states, which are defined by a canonical transformation that stepwise eliminates the hybridization between the f and c electrons.[37] The operator form of the effective QP Hamiltonian obtained in such a way is quadratic but the operator algebra is not fermionic. The charge and heat current density operators are highly nontrivial in the QP representation, and it is not clear that they satisfy the Jonson-Mahan theorem nor that the canonical expression in Eq. (11) for the Seebeck coefficient holds. To avoid these difficulties, we use the QP representation to estimate the Fermi momentum of the interacting system but calculate the heat and charge currents for the initial model, where the Jonson-Mahan theorem is easily proven.

B. Anderson model: "Poor man's approach"

At elevated temperatures, the FL law in Eq. (31) breaks down, and to obtain $\alpha(T)$ we need the full solution of the periodic Anderson model with the CF splittings and/or large degeneracy. Such a solution is not available at present and to estimate $\alpha(T)$ we use a poor man's approach. We assume that the conduction electrons scatter incoherently on the $4f$ ions and calculate the transport relaxation time in the T-matrix approximation. We write $\Sigma_c(k,\omega^+) \simeq n_i T_{kk}(\omega^+)$, where $T_{kk}(\omega^+)$ is the single-ion scattering matrix on the real axis, and, for the stoichiometric compounds, set the concentration of $4f$ ions to $n_i=1$. Since transport integrals are restricted to the Fermi window, we average $T_{kk}(\omega^+)$ over the FS and calculate $\tau(\omega)$ using Eq. (22).

In the case of a single scattering channel (no CF splitting) the vertex corrections to the T matrix vanish by symmetry and the conduction electron's self-energy in Eq. (22) is given by $\Sigma_c(\omega^+)=V^2 G_f(\omega^+)$, where $G_f(\omega^+)$ is the retarded Green's function of the effective $\mathcal{L}$-fold degenerate single impurity Anderson model. When the degeneracy is lifted by the CF splitting, the vertex corrections do not vanish, but we neglect them anyway and use

$$\Sigma_c(\omega^+) = \sum_{\Gamma} V_{k_F\Gamma} G_\Gamma(\omega^+) V_{\Gamma k_F}, \tag{32}$$

where $V_{\Gamma k_F}=\langle \Gamma | V | \mathbf{k} \rangle$ is the FS average of the matrix element for the scattering between the c electrons (in the $\mathbf{k}$ state) and the f state (belonging to the irreducible representation Γ), and $G_\Gamma(\omega^+)$ is the corresponding Green's function of the single impurity Anderson model with CF splitting.

As regards the validity of the poor man's approach, we point out that the DMFT+NRG solution[15] of the spin-1/2 Anderson lattice shows that the electrical resistance $\rho(T)$ increases rapidly and is very large at temperature T_K, where $\alpha(T)$ has a maximum. For $T \geqslant T_K/2$, the thermopower of the lattice model[15] is very similar to the exact results[23] obtained for the spin-1/2 Anderson impurity. This indicates that the poor man's approach can be used to describe the stoichiometric compounds at temperatures above $T_K/2$, provided the single impurity scattering is solved by methods that can deal with a large Coulomb correlation and the CF splitting.

The experimental results on the heavy fermion and valence fluctuators provide additional support for the poor man's approach. The data show that the residual resistance of ternary and quaternary compounds such as $EuCu_2(Ge_{1-x}Si_x)_2$, $CePt_{1-x}Ni_x$, and $YbIn_{1-x}Ag_xCu_4$ grows rapidly with x, and for $0.3 \leqslant x \leqslant 0.8$ the mean free path is reduced by disorder to about a single lattice spacing. In these random alloys, the electron propagation is incoherent even at $T=0$ and the single impurity model should apply down to the lowest temperatures. At low doping and in stoichiometric compounds, the impurity description breaks down at low temperatures where ρ_0 is small. However, in these systems $\rho(T)$ and $\alpha(T)$ grow rapidly with increasing temperature [room temperature (RT)] and attain large maxima at T_K^ρ and T_K, respectively. In the case of degenerate f states or small CF splitting, the data show[5,38,39] $T_K^\rho < T_K <$ RT, and for $T \geqslant T_K^\rho/2$ there is not much difference between the stoichiometric compounds and doped systems; i.e., the impurity model applies. For large CF splitting, $\rho(T)$ has two maxima: a low-temperature one at T_K^ρ and a high-temperature one at T_ρ. The thermopower also exhibits two maxima:[40] a low-temperature one at $T_K > T_K^\rho$ and a high-temperature one at T_S.

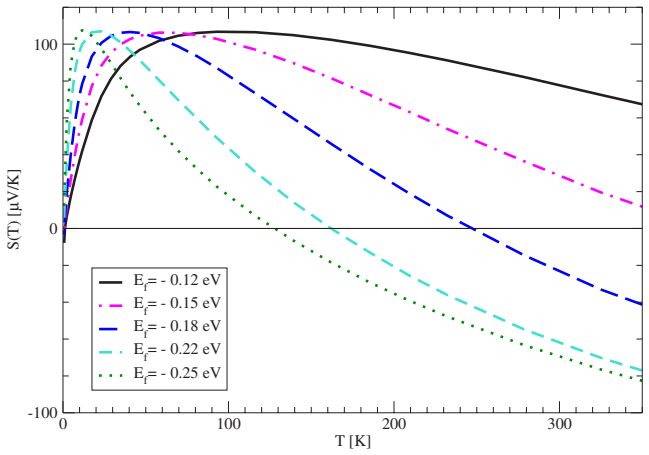

FIG. 1. (Color online) The thermopower of the single impurity Anderson model of an eight fold degenerate f state calculated by the NCA for fixed hybridization $\Gamma=0.015$ eV is plotted as a function of temperature for several values of E_f, as indicated in the figure. The values of $n_f(T_K)$ are 0.76, 0.81, 0.86 0.91, and 0.93 for $-E_f=0.12$, 0.15, 0.18, 0.22, and 0.25, respectively.

For $T \geqslant T_K/2$, where the mean free path is short, the thermopower of the periodic systems exhibits the same qualitative features as in random alloys and can be explained in terms of impurity scattering. The experimental data show that the functional form of $\alpha(T)$ is strongly affected by pressure or chemical pressure. The fact that all the qualitative features of the pressure-induced variations of $\alpha(T)$ can be successfully explained by impurity scattering justifies, *a posteriori*, the poor man's approach.

The thermoelectric properties of the single impurity Anderson model with the CF split f states are obtained by the NCA, which is explained in detail in Refs. 41 and 16. In the limit of large asymmetry and infinite f-f correlation, the Kondo temperature T_K, obtained from the low-energy peak of the spectral function, agrees with the exact result,[32] $T_K=3\gamma/\pi k_B$. Here, $\gamma=(\pi^2 k_B^2/3)\mathcal{L}\mathcal{N}_f(\mu)Z_f^{-1}$ is the impurity contribution to the specific heat coefficient, $\mathcal{N}_f(\mu)=(1/\pi\Gamma)\sin^2(\pi n_f/\mathcal{L})$ is the f-DOS at the Fermi level, and Z_f is the renormalization factor. For a structureless c-DOS, the NCA shows that T_K depends sensitively on the degeneracy of the f state. A small T_K is found for small $\mathcal{L}$ and large Δ_{CF}, while a large T_K is found for large $\mathcal{L}$ and small Δ_{CF}. For a given $\mathcal{L}$ and Δ_{CF}, the Kondo scale is a monotonic function of n_f. It has a minimum at $n_f=1$ and increases rapidly as n_f is reduced. In what follows, we discuss the behavior of $\alpha(T)$, assuming that pressure or doping increases the coupling constant g and reduces n_f but does not change Δ_{CF}.

We consider first an $\mathcal{L}$-fold degenerate f state and show typical NCA results[16,41,42] in Fig. 1, where thermopower is plotted as a function of temperature for several values of E_f. The calculations are performed for a half-filled, semielliptic c band, no CF splitting ($\mathcal{L}=8$), and a constant hybridization Γ. A decrease of E_f gives rise to an increase of g, which mimics the effect of pressure in Eu intermetallics. The thermopower is characterized by the Kondo maximum α_S at temperature $T_S \simeq T_K$. The high-temperature behavior strongly depends on the value of n_f. [Since n_f can be temperature dependent, we characterize the system by $n_f(T_K)$.] For $n_f \simeq 1$, the thermopower has a large high-temperature slope, changes sign at $T_0 > T_K$ and assumes large negative values above T_0. The T_S and T_0 increase, and the high-temperature slope of $\alpha(T)$ decreases with decreasing n_f. For $n_f < 0.7$, we still find a shallow maximum of $\alpha(T)$ below RT but the high-temperature slope is very small and the sign change does not occur. A similar behavior is obtained if the coupling constant g is reduced by increasing Γ. For smaller $\mathcal{L}$, we find the same qualitative features, but α_S and T_S are reduced; for $\mathcal{L}=2$ and $n_f \simeq 1$, the asymmetry of the model is much reduced and the Kondo maximum is almost completely suppressed.[40]

The CF splitting leads to additional features, which we explain by the example of an f ion with two CF states separated by Δ_{CF}. The respective degeneracies of the ground and the excited state are $\mathcal{M}$ and $\mathcal{M}'$, where $\mathcal{M}+\mathcal{M}'=\mathcal{L}$. The system now has two characteristic low-energy scales: the Kondo temperature T_K and a larger scale $T_K^{\mathcal{L}} \gg T_K$, which comes into play[43] when the excited CF states become significantly populated at temperature $T_\Delta \simeq \Delta_{\mathrm{CF}}/2$. For $T \geqslant T_\Delta$, the thermopower can be approximated by the function $\alpha_{\mathcal{L}}(T)$, which describes an effective $\mathcal{L}$-fold degenerate f state with the Kondo temperature $T_K^{\mathcal{L}}$ and exhibits all the features discussed in the previous paragraph. For $T < T_\Delta$, the excited CF states are unoccupied and the properties are determined by the lowest CF state, which is $\mathcal{M}$-fold degenerate (typically, $\mathcal{M} \ll \mathcal{L}$). Thus, the thermoelectric response of a CF split f level is described at low temperatures by an effective $\mathcal{M}$-fold degenerate Anderson model with the Kondo scale T_K. All other parameters being the same, the main difference between this effective model and a simple $\mathcal{M}$-fold degenerate model with the Kondo scale $T_K^{\mathcal{M}}=\lim_{\Delta\to\infty} T_K$ is that $T_K \gg T_K^{\mathcal{M}}$. The enhancement of T_K is due to the virtual transitions from the ground to the excited CF states. The function $\alpha_{\mathcal{M}}(T)$, which approximates $\alpha(T)$ at low temperatures, exhibits all the usual Kondo features. For $n_f \simeq 1$, it has a Kondo maximum at T_K and changes sign at $T_0 > T_K$; in the case of a doublet ground state, the Kondo maximum is very small and $\alpha(T)$ is negative down to the lowest accessible temperatures.[40] For $0.7 \leqslant n_f \leqslant 0.95$, the Kondo maximum is enhanced with respect to $n_f \simeq 1$, the high-temperature slope of $\alpha(T)$ is reduced, and the sign change shifts to $T_0 \gg T_K$. For $n_f \leqslant 0.7$, the maximum of $\alpha(T)$ is further enhanced but the sign change is absent. Of course, for $T \geqslant T_\Delta$, the excited CF states come into play and $\alpha_{\mathcal{M}}(T)$ ceases to be physically relevant.

These effects are illustrated for a ground state doublet and an excited quartet in Fig. 2, where $\alpha(T)$ is plotted as a function of temperature for various values of $\Gamma(p)$. The CF spitting Δ_{CF} is the same for all the curves. An increase of pressure increases $\Gamma(p)$ and $g(p)$ and reduces n_f, which has a drastic effect on the functional form of $\alpha(T)$. We assume at ambient pressure $n_f \simeq 1$ and choose $\Gamma(0)$ and $g(0)$ such that $\alpha(T) < 0$ at RT. The corresponding NCA spectral function has well defined CF excitations,[16,41] which show that the low-energy scales satisfy $T_K \ll T_K^{\mathcal{L}} \ll T_\Delta$. From the previous discussion, we expect $\alpha(T)$ with a very weak Kondo maximum at T_K, a sign change at $T_0 > T_K$, and large negative values for $T \gg T_0$. Nothing particular happens at $T \simeq T_K^{\mathcal{L}}$,

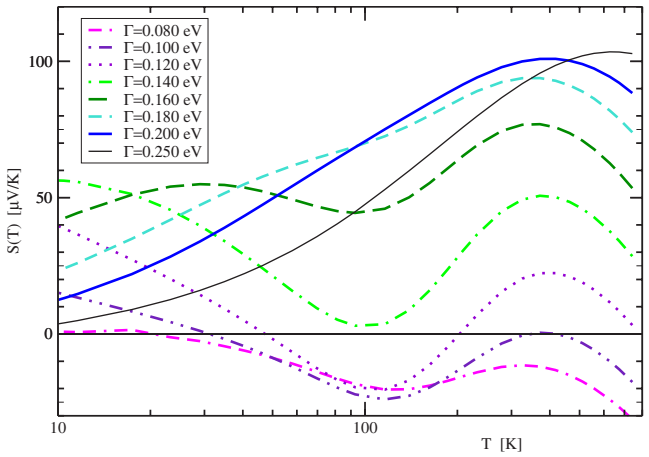

FIG. 2. (Color online) The thermopower of an f ion with the ground state doublet and excited quartet calculated by the NCA for the CF splitting $\Delta=0.07$ eV is plotted as a function of temperature for several values of the hybridization strength Γ, as indicated in the figure. The two bottom curves ($\Gamma=0.08,0.1$) describe the type (a) Kondo system, the third curve ($\Gamma=0.12$) from the bottom is type (b), the two middle curves ($\Gamma=0.14,0.16$) are type (c), and the third one from the top ($\Gamma=0.18$) describes the type (d) Kondo systems. The two upper curves $\Gamma=0.2,0.25$) (are type (e) and describe valence fluctuators.

where the excited CF states are still unoccupied. At T_Δ, the excited CF states become thermally populated and the functional form of $\alpha(T)$ changes from $\alpha_{\mathcal{M}}(T)$ to $\alpha_{\mathcal{L}}(T)$. Thus, a system with a low Kondo scale and large CF splitting has $\alpha(T)$ with a negative maximum around T_Δ and a deep negative minimum at low temperatures. The thermopower of that shape is illustrated by $\Gamma=0.08$ and $\Gamma=0.10$ curves in Fig. 2, classified[16,17] as type (a).

If $\Gamma(p)$ and $g(p)$ increase, such that $0.8\leqslant n_f\leqslant 0.95$, the NCA shows that the low-energy CF excitations are still resolved and $T_K(p)<T_K^{\mathcal{L}}(p)<T_\Delta$. In this parameter range, the Kondo maximum of $\alpha(T)$ is enhanced and shifted to higher temperatures, such that $\alpha_{\mathcal{M}}(p,T)>\alpha_{\mathcal{M}}(T)$ for $T\geqslant T_K(p)$. The values of T_K, $T_0(p)$, and $T_K^{\mathcal{L}}(p)$ are much closer to T_Δ than at ambient pressure, and $T_0^{\mathcal{L}}(p)$ is now above T_Δ. Thus, at the crossover we have $\alpha_{\mathcal{M}}(p,T)<0$ and $\alpha_{\mathcal{M}}(p,T)>0$. Since $\alpha_{\mathcal{L}}(p,T_\Delta)$ is enhanced with respect to the $p=0$ values, pressure enhances the Kondo maximum and brings it closer to the CF maximum. The temperature interval in which $\alpha(T)<0$ shrinks with pressure, while T_S does not change. These features are demonstrated by the $\Gamma=0.12$ curve in Fig. 2, which is classified as type (b).

In the pressure range such that $0.75\leqslant n_f\leqslant 0.8$ the sign change of $\alpha_{\mathcal{M}}(T)$ is pushed to even higher temperatures, and at large enough pressure (Γ) we eventually have $T_0(p)\geqslant T_\Delta$. The doublet-sextet crossover starts from $\alpha_{\mathcal{M}}(T_\Delta)\geqslant 0$, and $\alpha(T)$ exhibits two well resolved peaks, but is always positive. These features are demonstrated by the $\Gamma=0.14$ and $\Gamma=0.16$ curves in Fig. 2, which are classified as type (c). A further increase of pressure gives $0.7\leqslant n_f\leqslant 0.75$, which brings $T_K(p)$ so close to T_Δ that the Kondo and CF peaks cannot be resolved any more. The $\alpha(T)$ exhibits a single peak with a shoulder on the low-temperature side, as shown by the $\Gamma=0.18$ curve in Fig. 2, which is classified as type (d). Note that as long as the low-energy CF excitations are well defined, the thermopower has a peak at temperature $T_S\simeq T_\Delta$ and the magnitude of this peak increases with pressure.

If $\Gamma(p)$ and $g(p)$ become very large and n_f drops below 0.7, the spectral function will no longer show the CF excitations. The thermopower acquires a single maximum at T_S, which is unrelated to Δ_{CF}. The difference with respect to Kondo systems is that pressure shifts this thermopower peak to higher temperatures without changing its magnitude. Such behavior is typical of valence fluctuators and is demonstrated by the $\Gamma=0.20$ and $\Gamma=0.25$ curves in Fig. 2, which are classified as type (e). The curves in Fig. 1, which describe the system without the CF splitting such as Eu intermetallics, are also of this type. The Yb systems are characterized by an f hole, and the qualitative features of $\alpha(T)$ are obtained by reflecting ("mirror imaging") the curves in Fig. 1 or 2 on the temperature axis.

The NCA calculations break down for $T\ll T_K$, but an exact expression for the initial slope of the thermopower is easily obtained by the Sommerfeld expansion. This gives[23]

$$\lim_{T\to 0}\frac{\alpha(T)}{T}=\frac{2\gamma}{|e|n_c}\cot\left(\frac{\pi n_f}{\mathcal{L}}\right), \tag{33}$$

where $\mathcal{L}$ is the effective degeneracy of the f state at $T=0$. For Eu ions, $\mathcal{L}=8$. For the Ce and Yb ions with a small Kondo scale and large CF splitting, $\mathcal{L}$ is defined by the lowest CF state. If the CF splitting is removed by pressure or doping, we should use $\mathcal{L}=6$ for Ce and $\mathcal{L}=8$ Yb compounds. Since the on-site correlation is infinitely large and the model is far away from the electron-hole symmetry, the initial slope of $\alpha(T)$ is finite, even for the ground state doublet; it is positive for Ce and Eu ions, which have additional electrons in the magnetic configuration, and is negative for Yb ions, which are magnetic due to an additional hole. To estimate the magnitude of the initial slope, we have to take into account that γ decreases exponentially as $\mathcal{L}$ increases or n_f decreases. At constant $\mathcal{L}$, we find that $\alpha(T)/T$ decreases with the reduction of n_f, which is consistent with the NCA results shown in Fig. 1. For $\mathcal{L}=2$ and $n_f\simeq 1$, the slope of the thermopower becomes very small. Equation (33) shows that an increase of pressure or chemical pressure enhances the q ratio in disordered Ce alloys and reduces it in Yb alloys.

C. Falicov-Kimball model

In heavy fermions, the large paramagnetic entropy of the f ions is removed by the crossover to the FL phase with screened local moments. The Kondo screening does not affect n_f, which is nearly temperature independent. However, in some Eu and Yb systems, such as $EuCu_2Ni_2$ and $YbInCu_4$, the magnetic moment disappears due to a temperature-induced change in n_f; i.e., the entropy is reduced by a valence-change transition. These systems are described by the Falicov-Kimball model,[44] which takes a lattice of localized f sites, which can be either occupied or empty, and conduction states, which are delocalized via a nearest-neighbor hopping. The two types of electrons interact via a

short-range Coulomb interaction and share a common chemical potential, which controls the total number of electrons $n=n_c+n_f$. The occupation of the f states, which can be split into several CF levels, is restricted to $n_f<1$. For a given total number of electrons, thermal fluctuations change the average f occupation by transferring electrons or holes from the conduction band to the f states and vice versa.[27] The transport coefficients are obtained in the limit of infinite dimensions by substituting the exact conduction-electron Green's function into Eq. (13) and integrating Eq. (11) numerically.[28,45] This procedure allows us to discuss not only the dirty FL regime but also the metal-insulator transition.

To describe the $YbInCu_4$-like intermetallics, we assume that the Falicov-Kimball interaction is large enough to open a gap in the conduction band and the ground state is metallic, because μ is within the lower (or upper) Hubbard band. Since the model neglects quantum fluctuations, the ground state has no f holes and the conduction electrons are essentially free, such that $q\simeq 1$. At finite temperature, the $\mathcal{L}$-fold degenerate f states become fractionally occupied, and the additional paramagnetic entropy of these excited states competes for the free energy with the excitation energy, the kinetic energy of the conduction electrons, and the interaction energy.[44] This gives rise to a valence transition at a temperature T_V, such that a substantial number of electrons (in Eu compounds) or holes (in Yb compounds) are transferred from the conduction band to the $4f$ ions. The onset of the $4f$ paramagnetism is accompanied by the reconstruction of the interacting density of conduction states and the shift of μ into the gap.

We find[28,45] that the electrical resistance of the paramagnetic phase is large and has a maximum at a temperature $T^*\gg T_V$, which is of the order of the gap or the pseudogap in the density of states. The thermopower obtained by the DMFT is weakly temperature dependent, and its sign depends on the band filling. The maximum of $\alpha(T)$ is also at T^*. The overall entropy of the high-temperature phase is very large due to the contribution of local moments and $\tilde{q}\ll 1$. In systems with a valence-change transition, $\tilde{q}$ increases sharply to $q\simeq 1$ as temperature is reduced below T_V, indicating the onset of the free Fermi gas phase and the change of the Fermi volume. At intermediate temperatures, the behavior can be quite complex[28,45] because both the degeneracy of the f states and the number of charge carriers change at T_V.

By choosing the parameters of the model so as to increase the occupancy of the f states, one can stabilize the gapped phase, for large Coulomb repulsion, all the way down to zero temperature.[45] Calculating the thermopower for the spinless Falicov-Kimball model on a Bethe lattice gives[46] a thermopower that diverges as $\alpha(T)\simeq\Delta/T$, where Δ is the value of the gap. For an intrinsic semiconductor with a density of states increasing as a power law, and assuming that the frequency dependent conductivity is proportional to the density of states, we find[45] $\alpha(T)\simeq\ln T$. In both cases, the corresponding conductivity decays exponentially, so that the entropy current density generated by the applied field, $\mathcal{S}(T)=\alpha(T)\sigma(T)(-\nabla\phi)$, vanishes in the limit $T\to 0$, as required by the third law of thermodynamics.[12] This example shows that the value of the q ratio of a correlated insulator or semiconductor can become very large at low temperatures.

IV. DISCUSSION OF THE EXPERIMENTAL DATA

In this section, we use the results obtained for the periodic Anderson and the Falicov-Kimball models to discuss the temperature and doping dependence of $\alpha(T)$ and $\alpha/\gamma T$ for several typical intermetallic compounds with Eu, Ce, and Yb ions. In these compounds, chemical substitution modifies the character of the ground state, changes the characteristic temperature and the low-temperature values of $\alpha(T)/T$ and γ by an order of magnitude, and strongly modifies the temperature dependence of $\alpha(T)$, but does not significantly change the ratio $\alpha/\gamma T$. Our theory explains the universal low-temperature features and shows that the observed shapes of $\alpha(T)$ are consistent with the ground state properties at each doping level.

A. Chemical pressure effects in $EuCu_2(Ge_{1-x}Si_x)_2$

In $EuCu_2(Ge_{1-x}Si_x)_2$ intermetallics, Ge doping increases the lattice parameter and acts as a negative pressure, which reduces the coupling constant and makes the system more magnetic.[4,5] For $x\simeq 1$, the x-ray photoemission spectroscopy (XPS) data indicate a significant mixture of Eu^{2+} and Eu^{3+} ions typical of a valence fluctuator. The spectral weight of the nonmagnetic Eu^{3+} configuration decreases with respect to the weight of the magnetic Eu^{2+} configuration as x is reduced. At the critical concentration $x_c=0.65$, there is a change from a FL to an antiferromagnetic (AFM) ground state. The XPS shows that the weight of the Eu^{3+} configuration continues to decrease in the magnetic phase and becomes undetectable only for $x\leqslant 0.3$.

In $EuCu_2Si_2$, the initial slope of $\alpha(T)$ is small, $\alpha/T=0.64\ \mu V/K^2$, the specific heat has a small linear coefficient, $\gamma=0.065\ J/K^2$ mol, and the q ratio[5] is $q|_{x=1}=0.94$. For $0.90\geqslant x\geqslant 0.65$, the γ value increases with Ge doping and $x=0.7$ gives $\alpha/T=2.86\ \mu V/K^2$, $\gamma=0.226\ J/K^2$ mol, and $q|_{x=.7}=1.21$. The doping dependence of the q ratio for $x>x_c$ can be explained by the periodic Anderson model, which takes into account the eightfold degeneracy of the Eu^{2+} ions but neglects the excited magnetic states of the Eu^{3+} configuration. The slight enhancement of $q(x)$ obtained for $x_c<x<1$ is most likely due to the transfer of electrons from the conduction band into the f level induced by a negative chemical pressure. The observed trend agrees with Eq. (31), which predicts that a reduction of the charge carrier density increases the q ratio. It seems that $q(x)$ increases more rapidly as we approach the AFM transition from the paramagnetic side, but the concentration dependence would have to be fine-tuned before a more quantitative conclusion could be reached.

Doping not only changes the ground state from the paramagnetic to the AFM one but affects the overall shape of $\alpha(T)$. These modifications are very well described by the NCA calculations for an eightfold degenerate single impurity Anderson model.[42] Note that since $\rho(T)$ is very large for $T\geqslant T_K/2$, the poor man's approach applies. The experimental data exhibit all the qualitative features shown in Fig. 1,

where the curves with the highest T_S and lowest n_f correspond to the Si-rich compound and those with the lowest T_S and $n_f \simeq 1$ correspond to Ge-rich samples. (Figure 1 captures the qualitative features of the experimental data, but the quantitative analysis has to take into account the nonresonant scattering channels and the Nordheim-Gorter rule.)

For $x \simeq 1$, the maximum of $\alpha(T)$ occurs at the highest temperatures ($T_S \simeq 150$ K) and no sign change of $\alpha(T)$ is observed. This is consistent with the mixed-valent character of the Eu ions, as indicated by the XPS data. For $0.9 \leqslant x \leqslant 1$, the thermopower is always positive and reaches a broad maximum, $\alpha_S > 40$ μV/K, at about $T_S \geqslant 125$ K. The value of α_S does not change much as x decreases, but T_S is reduced and the low-temperature slope of $\alpha(T)$ is enhanced with Ge doping. (See the full and dashed-dotted lines in Fig. 1.) A further increase of Ge concentration shifts the maximum of $\alpha(T)$ to lower temperatures, increases the low- and high-temperature slopes of $\alpha(T)$, and gives rise to the sign change at $T_0(x)$; the Ge doping reduces $T_0(x)$ faster than $T_S(x)$. These changes are in complete agreement with the pressure effects discussed in Sec. III B. (See the dashed and dotted lines in Fig. 1.) The comparison between the theory and experiment allows us to identify $T_S(x) = T_K(x)$ and associate the decrease of $T_0(x)$ with the enhanced magnetic character of the Eu ions due to the reduced f-c coupling.

For $x < x_c$, long-range magnetic order occurs at the Neel temperature $T_N(x)$, as indicated by an anomaly in $C_P(T)$ and a discontinuity in the slope of $\rho(T)$.[4,5] The magnetic transition is difficult to see in the $\alpha(T)$ data for $0.6 < x \leqslant x_c$. In this concentration range, the Ge doping increases T_N, reduces T_K, and sharpens the maximum of $\alpha(T)$. This maximum is fully developed, T_K is close to T_N, and the only effect of the AFM transition on $\alpha(T)$ is a slight change of slope at T_N. For $0.5 \leqslant x \leqslant 0.6$, a negative pressure reduces $T_K(x)$ below $T_N(x)$, such that $\alpha(T_N) < \alpha_S$ and $\alpha(T)$ acquires a cusp. The reason is that the slope of $\alpha(T)$ is negative for $T > T_N > T_K$ and positive for $T < T_N$, which gives rise to a cusp at T_N. However, $T_N(x)$ is still rather close to $T_K(x)$ and the values of $\alpha(T)$ around $T_N(x)$ are large. Nonetheless, the cusp makes the overall shape of $\alpha(T)$ quite different from what one finds in samples with a FL ground state, where $\alpha(T)$ has a rounded maximum (see Figs. 4 and 7 in Ref. 5). The shape of $\alpha(T)$ for temperatures above $T_N(x)$ looks very much the same as in the nonmagnetic samples well above T_S; i.e., $\alpha(T)$ decreases monotonically and changes sign at $T_0(x)$ (see Fig. 6 of Ref. 5). The single impurity Anderson model allows us to infer $T_K(x)$ from the shape of $\alpha(T)$ and follow the concentration dependence of $T_K(x)$ even for samples in which $T_K(x) \ll T_N(x)$. For $x \leqslant 0.5$, the Ge doping reduces $T_K(x)$ much faster than $T_N(x)$, and the AFM transition occurs at temperatures comparable to $T_0(x)$. The thermopower anomaly at T_N is now very weak because the Kondo screening is small ($T_N \gg T_K$), and the data are taken at temperatures much higher than T_K. (The thermopower in the paramagnetic phase is always far away from the Kondo maximum.)

The overall temperature and concentration dependence of $\alpha(T)$ and $C_V(T)$ in the AFM samples indicate that $T_N(x)$ increases rapidly from zero as x is reduced below x_c. The low-temperature maxima of $\gamma(x)$ and αT are at $x_c = 0.65$, while the maximum of $T_N(x)$ is reached for $x \simeq 0.5$. Below this concentration $T_N(x)$ decreases slowly as x is reduced.[4] Such a behavior is difficult to explain in terms of the simple Doniach diagram, which considers the scattering of conduction electrons on a lattice of localized spins and predicts that $\gamma(x)$ and $T_N(x)$ should peak at x_c. If we assume that the thermopower tracks the entropy of the charge carriers, the large values of $\alpha(T)$ found for $0.55 \leqslant x \leqslant 0.65$ point to a large hybridization below T_N, which agrees with the XPS data. In this concentration range, the Kondo scale is comparable to T_N and the magnetic order sets in before the paramagnetic entropy is quenched by the Kondo effect. For these samples, the paramagnetic entropy is removed at T_N by an anomalous spin density wave (SDW), which gaps a part of the hybridized FS. Indirect evidence for the SDW transition is provided by the large specific heat and small effective moment in the ordered phase. Direct evidence by neutron scattering data on $EuCu_2(Ge_{1-x}Si_x)_2$ is lacking, but the SDW transition has been seen recently in high-pressure neutron data[47] on the "reduced-moment" antiferromagnet $CePd_2Si_2$. (Unfortunately, the high-pressure thermopower and the specific heat data on this compound are not available.) The smaller values of $\alpha(T)$ found for $x < 0.5$ indicate a reduced f-c coupling due to negative chemical pressure. At the Ge-rich end, the hybridization and the Kondo coupling are negligibly small and the f electrons are completely localized. For $x \leqslant 0.3$, the magnetic ground state involves the unscreened local moments of the Eu^{2+} ions. Below T_N, the conduction states are effectively free, except for scattering off spin waves. The low-temperature entropy is dominated by the linear conduction-electron contribution, and $\alpha(T)$ is too small to show an anomaly at T_N. Thus, we take the thermopower data as an evidence for different magnetic ground states in $x \simeq x_c$ and $x = 0$ samples.

B. Chemical pressure effects in $CePt_{1-x}Ni_x$ intermetallics

For our next example, we consider the doping effects on $\alpha(T)$ and $\alpha/\gamma T$ in $CePt_{1-x}Ni_x$. For $x \geqslant 0.95$, this system is a valence fluctuator with a FL ground state, and for $x < 0.95$, a heavy fermion with a ferromagnetic (FM) ground state.[6,7,48] The temperature and concentration dependence of $\alpha(T)$ in the paramagnetic phase shows all the typical features of a Ce ion with a CF split f state, as discussed in detail in Sec. III B. The CF splitting is estimated to be about 200 K and $T_\Delta \simeq 100$ K.[48] We account for the observed behavior, assuming that the expansion of the volume due to Pt doping[48] reduces the hybridization and the effective coupling constant but does not change Δ_{CF}. The qualitative features of the thermopower agree with the schematic results shown in Fig. 2, but for a quantitative agreement we should use the appropriate CF scheme and tune the model parameters. Also, the systematic analysis of the q ratio for samples with the FL ground state is difficult because it would require the data in a very narrow concentration range, $0.95 \leqslant 1$.

For $0.9 \leqslant x < 1$, the thermopower is linear at low temperatures, shows a maximum α_S at $T_S \simeq 120$ K and a slow decay of $\alpha(T)$ above T_S. The Pt doping reduces T_S to 100 K with-

out a significant change in α_S, which can be compared with the type (e) curves in Fig. 2. Such behavior is typical of valence fluctuators in which n_f is too small for the CF excitations to appear. We estimate the initial slope of $\alpha(T)$ for $x=0.95$ to be about[6] $\alpha/T \simeq 3\ \mu\mathrm{V/K}^2$ and the specific heat coefficient to be $\gamma=0.120\ \mathrm{J/K}^2\ \mathrm{mol}$,[7] which gives $q|_{0.95} \simeq 2.4$.

For $0.75 \leqslant x \leqslant 0.95$, the experimental data show a new feature: $\alpha(T)$ assumes first shape (d) and then (c). In this concentration range, Pt doping reduces α_S but does not change T_S, which indicates the presence of CF excitations and two (or more) low-energy scales. The high-temperature scale $T_K^{\mathcal{L}}$ characterizes a fully degenerate CF state, and the low-temperature one, T_K, characterizes the CF ground state. To explain the data, we assume $T_K < T_K^{\mathcal{L}} < T_0 \simeq T_\Delta$, which requires large coupling and $n_f < 1$ (see the discussion in Sec. III B). At RT, all the CF states are equally populated, the f state is effectively sixfold degenerate ($\mathcal{L}=6$), and $\alpha(T)$ can be approximated by $\alpha_{\mathcal{L}}(T)$, which has a negative RT slope. As temperature decreases, the excited CF states depopulate, and at T_Δ there is a crossover from the high-temperature regime to the low-temperature one, where the f state is an effective doublet ($\mathcal{M}=2$) and $\alpha(T) \simeq \alpha_{\mathcal{M}}(T)$. Since $n_f < 1$, T_0 is comparable to T_Δ and the crossover is indicated only by a small change in the slope of $\alpha(T)$. Negative chemical pressure shifts $T_K^{\mathcal{L}}$ to lower temperatures and reduces the values of $\alpha_{\mathcal{L}}(T)$ for $T > T_K^{\mathcal{L}}$. These features explain the reduction of the high-temperature maximum of $\alpha(T)$ by Pt doping. [Since Δ_{CF} does not change by doping and $T_S \simeq T_\Delta \gg T_K^{\mathcal{L}}$, the maximum $\alpha_S(x)$ is always at T_Δ.] The peculiar feature of $CePt_{1-x}Ni_x$ in this concentration range is the FM transition, which occurs at $T_c \simeq T_K$ and is indicated by the discontinuous change in the slope[6,48] of $\alpha(T)$ and $\rho(T)$. [This feature is quite similar to what one finds at the AFM transition in $EuCu_2(Ge_{1-x}Si_x)_2$.] At $x=0.85$, the thermopower and the specific heat data give $\alpha/T \simeq 4\ \mu\mathrm{V/K}^2$ (Ref. 6) and $\gamma = 0.180\ \mathrm{J/K}^2\ \mathrm{mol}$,[7] such that $q|_{0.85} \simeq 2.1$. Using Eq. (31), one is tempted to associate the reduction of $q(x)$ by Pt doping with the transfer of f electrons into the conduction band. However, the onset of the FM transition makes the estimate of the initial thermopower and the specific heat slope susceptible to large errors, and a quantitative analysis is difficult. The low-temperature entropy is now due to the magnetic degrees of freedom and is unrelated to the entropy of the charge carriers.

A further increase in the Pt concentration continuously reduces the f-c coupling and brings n_f closer to 1, which makes Ce more magnetic. The T_K and T_0 shift rapidly to lower temperatures, such that $T_0 < T_\Delta$ for $x \simeq 0.5$. Once the high- and low-temperature regimes are sufficiently far apart, a double-peak structure appears in $\alpha(T)$. The high-temperature peak remains at $T_S(x) \simeq T_\Delta$, but its magnitude $\alpha_S(x)$ is systematically reduced by Pt doping. Considered as a function of temperature, $\alpha(T)$ goes through a minimum for $T < T_S$, and then increases toward the Kondo maximum α_K, as predicted by the NCA calculations. The minimum of $\alpha(T)$ for $x=0.5$ does not reach negative values [compare with the type (c) curve in Fig. 2]. For $x < 0.5$, there is a range of temperatures for which $\alpha(T) < 0$; i.e., the type (b) behavior is obtained. The data show that $T_0(x)$ decreases rapidly with Pt doping, but the corresponding shift of α_K cannot be seen because the development of the Kondo peak of $\alpha(T)$ is intercepted by the FM transition. Instead of a Kondo peak, we find $\alpha(T)$ with a cusp at T_c, which is similar to the one seen in $EuCu_2(Ge_{1-x}Si_x)_2$ for $x \leqslant 0.5$. The onset of the magnetic transition below T_K and the nonmonotonic concentration dependence of $T_c(x)$ are difficult to understand in terms of the Doniach diagram, obtained by a simple comparison of the Kondo and the Ruderman-Kittel-Kasuya-Yosida (RKKY) scales. The large values of $\alpha(T)$ at the transition and the similarity to the $EuCu_2(Ge_{1-x}Si_x)_2$ data can be taken as evidence of a large Fermi volume that comprises the f states. The ferromagnetic transition in $CePt_{1-x}Ni_x$ samples with $0.5 \leqslant x \leqslant 0.95$ is due to an anomalous SDW transition, which partly gaps the hybridized FS. On the other hand, in the Pt-rich samples, $x < 0.5$, the small values of $\alpha(T)$ indicate the localized f states and the conduction band with a small Fermi volume. As in $EuCu_2(Ge_{1-x}Si_x)_2$, the thermopower data indicate different magnetic ground states of the Ni-rich and Pt-rich samples.

A similar behavior for $\alpha(T)$ is also seen in many other Ce intermetallics such as $Ce(Pb_{1-x}Sn_x)_3$ and $Ce(Cu_{1-x}Ni_x)_2Al_3$,[3] in which the $\alpha/\gamma T$ ratio is about twice as large as in $EuCu_2(Ge_{1-x}Si_x)_2$. It would be interesting to study the q ratio as one approaches the critical concentration from the paramagnetic side and determine whether $q(x)$ exhibits different features above the AFM and the FM transitions.

C. Chemical pressure effects in Ag-rich $YbIn_{1-x}Ag_xCu_4$

Another example of chemical pressure effects is provided by $YbIn_{1-x}Ag_xCu_4$ intermetallics,[8,9,18] which show an anomalous behavior due to the fluctuations of Yb ions between the magnetic Yb^{3+} configuration with a single f hole and the full f-shell Yb^{2+} configuration. Indium doping expands the lattice and increases the weight of the Yb^{2+} with respect to the Yb^{3+} configuration[19] by transferring electrons from the conduction band to the $4f$ state. This reduces the number of f holes and increases the Kondo coupling, which makes the compound less magnetic. However, the depletion of the conduction band due to chemical pressure is compensated by the substitution of the monovalent Ag by the trivalent In. (The total number of conduction electrons increases with In doping.)

We consider first the behavior of these compounds in the coherent FL regime. $YbAgCu_4$ is a typical heavy fermion with a small characteristic temperature,[9,18] as indicated by an enhanced Pauli-like magnetic susceptibility, a large specific heat coefficient, and a large concentration of Yb^{3+} ions. Resonant inelastic x-ray scattering (RIXS) data show[50] the presence of f holes in the ground state at the Ag-rich end. The thermopower and specific heat data give $\alpha/T = 2.2\ \mu\mathrm{V/K}^2$ and $\gamma = 0.215\ \mathrm{J/K}^2\ \mathrm{mol}$ at $T \leqslant 10$ K, such that $q|_{x=1} = 0.98$. At the In-rich end ($x \leqslant 0.4$), the system is a typical valence fluctuator with a large characteristic temperature, as indicated by the slowly varying metallic resistivity, weakly enhanced Pauli-like susceptibility, and small specific heat coefficient.[49] The x-ray absorption data[18] indicate that

$n_f^h < 0.9$ in the ground state, i.e., a reduced weight of the $4f^{13}$ configuration. For $x=0.4$, the thermopower and specific heat data at 10 K give $\alpha/T=0.36\ \mu V/K^2$ and $\gamma=0.036\ J/K^2$ mol, such that $q|_{x=.4}=0.96$. For $0 \leqslant x \leqslant 0.4$, the values of α and γ in the FL regime do not show any further changes with doping. Describing the Ag-rich compounds by the periodic Anderson model, we find that the doping dependence of q is consistent with Eq. (31) if we take into account that the Ag-In substitution increases the number of conduction electrons despite the charge transfer induced by the negative chemical pressure. Thus, In doping transforms the system from a heavy fermion into a valence fluctuator and changes the low-temperature value of γ and α/T by an order of magnitude but has only a small effect on the low-temperature ratio $\alpha/\gamma T$. The enhanced thermopower slope and large specific heat coefficient indicate a large Fermi volume due to the hybridized f states.

The temperature dependence of $\alpha(T)$ is consistent with the ground state properties for each value of x. To start with, notice that the electrical resistance of all these compounds increases rapidly with temperature or doping and that above the FL regime the mean free path is short enough to justify the poor man's approach. (For $0.3 \leqslant x \leqslant 0.8$, the residual resistivity is large and the single impurity approach can be extended down to $T=0$; i.e., the translationally invariant FL of the periodic system can be replaced by the local FL.) The properties of the stoichiometric compound $YbAgCu_4$ above the FL regime are well described by the NCA solution of a CF split Anderson model with a ground state doublet, and excited quartet and doublet states at 4 and 7 meV, respectively.[50] Taking the coupling $g=V^2\mathcal{N}_0(\mu)/|E_f-\mu|$, such that $T_K=70$ K, we find the ground state value $n_f^h \simeq 0.9$ and the temperature variation $n_f^h(T)$, which agree with the RIXS data.[50] For the same parameters, the NCA calculations give $\alpha(T)$ with a deep negative minimum of about $\alpha_S \simeq -30\ \mu V/K$ and $T_S \simeq 60$ K. The CF splitting is too small (or g is too large) to produce any discernible CF structure, and the overall shape of $\alpha(T)$ is characterized by a single deep minimum. [Note the mirror image analogy with the intermetallic compounds with Ce ions: $\alpha(T)$ is described by the mirror image of the type (d) curve in Fig. 2.] The NCA results agree with the experimental data on $YbAgCu_4$, which show[9] $\alpha(T)$ with a broad minimum at about $T_S \simeq 50$ K and $\alpha_S \simeq -40\ \mu V/K$. Above T_S, the thermopower has a large positive slope, which is consistent with $n_f^h \simeq 0.9$ and reaches small negative values at RT. For $T \gg T_K$ the f electrons are localized and contribute a large paramagnetic term to the overall entropy (the entropy of the unhybridized conduction electrons is small), so that $\tilde{q} \ll 1$.

For $0.5 \leqslant x \leqslant 1$, the experimental data show[9] that In doping shifts $\alpha(T)$ to higher temperatures, such that $T_S(x) > T_S(0)$. The RT values are reduced by doping [$\alpha(T)$ is more negative], but the bare data show $\alpha_S(x) > \alpha_S(0)$. The NCA calculations refer to the magnetic ion contribution, and a quantitative comparison would require the Nordheim-Gorter analysis, which cannot be performed since the absolute values of $\rho_0(x)$ are not available. The qualitative features of $\alpha(T)$ in the In-doped samples can be explained by the Anderson model with the same CF level scheme as for $YbAgCu_4$, but with an enhanced coupling. The negative chemical pressure due to In substitution shifts the bare f level closer to the chemical potential but does not change the hybridization. (For details of the NCA description of Yb compounds, see Ref. 16.) Thus, replacing Ag by In enhances $g(x)$ and large enough doping gives $g(x) \simeq 1$, such that $YbIn_{1-x}Ag_xCu_4$ becomes a valence fluctuator. The NCA solution shows that an increase of $g(x)$ enhances $T_K(x)$ and $T_S(x)$ with respect to the $x=0$ values and reduces the slope of $\alpha(T)$ above $T_S(x)$. This makes the RT values of $\alpha(T)$ more negative, in agreement with experiment.[9] Using the mirror image analogy with Ce compounds, we see in Fig. 2 that In doping transforms the type (d) thermopower of a heavy fermion with large T_K into the type (e) thermopower of a valence fluctuator.

D. Chemical pressure effects in the In-rich $YbIn_{1-x}Ag_xCu_4$

For $x \leqslant 0.5$, the substitution of monovalent Ag by trivalent In brings μ and E_f in the vicinity of the band edge E_c, which gives rise to completely new features. The $n_f^h(T)$ becomes strongly temperature dependent, and the temperature-induced transfer of f holes from the conduction band can reduce $\mu - E_c$ and $E_f - E_c$ to zero. Once μ is within the gap of the density of states, the effective hybridization is switched off and the magnetic moment of the f ions cannot be quenched by Kondo screening;[51,52] i.e., the paramagnetic entropy of the high-temperature phase cannot be removed by the Kondo effect. Thus, the transition from the high-temperature disordered paramagnetic state to the low-temperature coherent FL state cannot follow the usual "Kondo route" taken by the heavy fermions. The valence fluctuators such as $YbIn_{1-x}Ag_xCu_4$ for $x \leqslant 0.5$, belong to a new class of materials in which the transition between the low- and high-entropy phases is driven by the Falicov-Kimball interaction. This gives rise, at the temperature T_V, to a change in the relative occupancy of the f and the conduction states and to an abrupt modification of the properties of the system. The valence-change transition is clearly seen in the x-ray absorption data; above T_V, the spectra indicate a stable $4f^{13}$ configuration of Yb ions, and below T_V, one has a mixture of $4f^{13}$ and f^{14} states.[18] The magnetic character of the Yb ions changes at T_V, as indicated by an abrupt change of the susceptibility from Pauli-like to Curie-like.[18] In the high-temperature phase, the Curie constant is close to the free ion value of Yb^{3+}. The conduction states are also modified at T_V, as indicated by a drastic change of the frequency dependence of the optical conductivity[53] and by a large increase in the resistivity.[54] The electrical resistance and the Hall coefficient of the high-temperature phase of $YbIn_{1-x}Ag_xCu_4$ are typical of narrow-band semiconductors or semimetals with a very low carrier density, and neither the transport nor the thermodynamic properties show any sign of the Kondo effect. The proximity of μ to E_c is indicated in $YbInCu_4$ by the Hall data and band-structure calculations.[54]

The anomalous thermoelectric response of f electrons close to the metal-insulator transition, which characterizes the $YbInCu_4$-like systems, is well described by the spin-degenerate Falicov-Kimball model.[44] Performing DMFT calculations for a parameter set that yields the valence-change

transition at $T_V=50$ K and opens a pseudogap of the order of $T^* \simeq 500$ K, we obtain the main features of the magnetic susceptibility, the XPS data, and the optical conductivity of $YbIn_{1-x}Ag_xCu_4$ at temperatures above T_V. The calculated thermopower[28] is of the order of a few $\mu V/K$, and its sign is either positive or negative, depending on the band filling and the shape of the conduction band. The proximity of μ to the pseudogap would lead (in a noninteracting system) to a shallow minimum of $\alpha(T)$ at a temperature of the order of T^*, but in an interacting system, the valence-change transition destabilizes the semiconducting phase and gives rise to a discontinuity of $\alpha(T)$ at T_V. The low-temperature FL state has a large characteristic temperature, and $\alpha(T)$ is a linearly decreasing function of temperature; its slope is given by Eq. (31). Thus, a cusp or even a discontinuity appears in $\alpha(T)$ at T_V. Below T_V, the entropy of the system is given by the entropy of the conduction states and $q=1$. Above T_V, the entropy is dominated by the contribution of the localized, paramagnetic states, $\mathcal{S} \simeq R \ln 8$, and $\tilde{q} \ll 1$. The large jump of the $\alpha/\mathcal{S}$ ratio at T_V is an indication of the temperature-induced change in Fermi volume.

V. SUMMARY AND CONCLUSIONS

In this contribution, we have discussed recent experiments on the universal ratio of the low-temperature thermopower and specific heat of heavy fermions and valence fluctuators with Ce, Eu, and Yb ions.[1–9,48] The experimental data have shown[1,2] that systems with very different values of α/T and γ often have similar values of the low-temperature ratio $q=N_A e\alpha(T)/\gamma T$. Here, we considered in some detail the $EuCu_2(Ge_{1-x}Si_x)_2$, $CePt_{1-x}Ni_x$, and $YbIn_{1-x}Ag_xCu_4$ intermetallics, in which the character of the ground state is concentration dependent and α/T and γ change by an order of magnitude, while $q(x)$ shows only small, but systematic, deviations from universality. Doping or pressure not only affects the slope but also alters the overall shape of $\alpha(T)$; these changes follow a well established pattern[11,16,17] that depends on the relative magnitude of the Kondo scale and CF splitting.

We have first approached the thermoelectric response of the above mentioned systems on a macroscopic level and derived the $\alpha/\gamma T$ ratio from transport equations. Using general thermodynamic arguments and assuming that charge and heat are transported at low temperatures by quasiparticle currents, we found $q=N_A/N$, where N/N_A is the effective concentration of the charge carriers. This derivation has also shown that for a general many-body system, the $q=N_A/N$ law is only approximately valid. We have discussed various possible sources of the nonuniversal behavior and have pointed out the difficulties that one encounters when comparing the experimental and theoretical results for systems that are close to a phase boundary.

On a microscopic level, we have analyzed the behavior of the periodic Anderson and the Falicov-Kimball models using the DMFT approach. We have discussed two possible routes that the system can follow to remove the entropy of the paramagnetic states at low temperatures (the Kondo and the Falicov-Kimball route) and have shown that in both cases the ratio of the thermopower and the entropy, $\alpha/\mathcal{S}$, tracks the Fermi volume of the charge carriers. In the FL regime, we find that the $\alpha/\gamma T$ ratio is given by the expression in Eq. (31), which explains the near universality of the q ratio in $EuCu_2(Ge_{1-x}Si_x)_2$, $YbIn_{1-x}Ag_xCu_4$, and similar systems. A weak concentration dependence of $\alpha/\gamma T$ is most likely due to the transfer of charge from the f level to the conduction band or vice versa, as described in Eq. (31). The $CePt_{1-x}Ni_x$ data also show a slight doping dependence, but the onset of the ferromagnetic transition at relatively high temperatures precludes a quantitative analysis. Calculations for correlated electrons close to the metal-insulator transition, described by the Falicov-Kimball model, show that the q ratio can assume very large values at low temperatures.

In the case of random alloys described by the single impurity Anderson model, the zero-temperature limit of $\alpha/\gamma T$ is given by the expression in Eq. (33), which differs by $\cot(\pi n_f/\mathcal{L})$ from the corresponding expression in Eq. (31) for the Anderson lattice. Here, the q ratio has an explicit dependence on the effective degeneracy of the f electron ground state. This result applies to substitutional alloys obtained by doping the rare earth sites, such as $Ce_{1-x}La_xB_6$,[38,39] $Ce_{1-x}Y_xCu_2Si_2$,[55] $Ce_{1-x}La_xCu_2Si_2$,[56] $Yb_{1-x}Y_xInCu_4$,[57] and similar systems. It might also apply to ternary and quaternary systems with one rare earth ion per unit cell but a short mean free path due to disorder. Equations (31) and (33), combined with the charge neutrality condition $n=n_f+n_c$, predict different pressure dependences of the q ratio for periodic systems and random alloys. The experimental verification regarding the "universality" of the $\alpha/\gamma T$ ratio is complicated by the fact that the magnetic and nonmagnetic contributions to $\alpha(T)$ and $C_V(T)$ are often difficult to separate. The situation could be improved by performing the transport and thermodynamic measurements at various hydrostatic pressures on the same samples. It would also be interesting to follow the behavior of the q ratio as the system approaches a magnetic or a metal-insulator transition, which gives rise to the changes in the Fermi volume.

The temperature dependence of $\alpha(T)$ has been calculated using a poor man's approach, which describes the scattering of c electrons on the lattice of f ions by the single impurity Anderson model with CF splitting. This provides an accurate description for intermetallic compounds with one $4f$ ion per unit cell when the mean free path is sufficiently reduced by a thermal or a substitutional disorder. The solution shown in Figs. 1 and 2 captures all the qualitative features of $\alpha(T)$ observed in $EuCu_2(Ge_{1-x}Si_x)_2$, $CePt_{1-x}Ni_x$, and $YbIn_{1-x}Ag_xCu_4$ intermetallics[1,3,4,6,8,9] for $T \geqslant T_K/2$. The scattering of c electrons on f states with CF splitting explains the double-peak structure found in many heavy fermions. The single-peaked $\alpha(T)$ of valence fluctuators is an indication of the absence of CF excitations. The overall temperature dependence of $\alpha(T)$ in periodic systems is obtained by interpolating between the poor man's (NCA) solution and the coherent FL (DMFT) solution given by Eq. (31). In random alloys, the low-temperature behavior is described by a local FL and $\alpha(T)$ is obtained by interpolating between Eq. (33) and the NCA result. We have found that the shape of $\alpha(T)$ depends on the relative magnitude of T_K, $T_K^{\mathcal{L}}$, and T_Δ and

have explained the seemingly complicated behavior of $\alpha(T)$ in a simple way.

Pressure and doping can remove the Kondo resonance from the spectral function and transform it into a broad structure typical of valence fluctuators. This changes the effective degeneracy of the f state and increases (or decreases) the characteristic temperature of a given compound by several orders of magnitude. Temperature can also change the degeneracy of the f state by populating the excited CF states. Since T_K and $T_K^{\mathcal{C}}$ are strongly pressure dependent, while T_Δ is not, the thermopower is drastically modified by pressure and doping. The thermopower measurements probe the low-energy excitations of the system and reveal important low-energy scales. We hope that our work motivates experimentalists to measure the thermopower and specific heat of single crystal heavy fermion under hydrostatic pressure.

ACKNOWLEDGMENTS

This work has been supported by the Ministry of Science of Croatia (MZOS, Grant No. 0035-0352843-2849), the COST P-16 ECOM project, the DFG (Grant No: Dr274/10-1), and the National Science Foundation (Grant No. DMR-0210717). Discussions with Z. Hossain, C. Geibel, J. Sakurai, D. Logan, F. Anders, K. Behnia, J. Flouquet, I. Aviani, M. Očko, and B. Horvatić are gratefully acknowledged.

[1] J. Sakurai, in *Transport and Thermal Properties of f-electron Systems*, edited by H. Fujii, T. Fujita, and G. Oomi (Plenum, New York, 1993), p. 165.
[2] K. Behnia, D. Jaccard, and J. Flouquet, J. Phys.: Condens. Matter **16**, 5187 (2004).
[3] J. Sakurai and Y. Isikawa, J. Phys. Soc. Jpn. **74**, 1926 (2005).
[4] S. Fukuda, Y. Nakanuma, J. Sakurai, A. Mitsuda, Y. Isikawa, F. Ishikawa, T. Goto, and T. Yamamoto, J. Phys. Soc. Jpn. **72**, 3189 (2003).
[5] Z. Hossain, C. Geibel, N. Senthilkumaran, M. Deppe, M. Baenitz, F. Schiller, and S. L. Molodtsov, Phys. Rev. B **69**, 014422 (2004).
[6] J. Sakurai, A. Iwasaki, Q. Lu, D. Ho, Y. Isikawa, J. R. Fernández, and C. Gómez Sal, J. Phys. Soc. Jpn. **71**, 2829 (2002).
[7] J. I. Espeso, J. C. Gómez Sal, and J. Chaboy, Phys. Rev. B **63**, 014416 (2000).
[8] M. Očko, Dj. Drobac, J. L. Sarrao, and Z. Fisk, Phys. Rev. B **64**, 085103 (2001).
[9] M. Očko, J. L. Sarrao, and Ž. Šimek, J. Magn. Magn. Mater. **43-46**, 284 (2004).
[10] H. Wilhelm and D. Jaccard, Phys. Rev. B **66**, 064428 (2002).
[11] H. Wilhelm, D. Jaccard, V. Zlatić, R. Monnier, B. Delley, and B. Coqblin, J. Phys.: Condens. Matter **17**, S823 (2005).
[12] E. M. Lifshitz, L. D. Landau, and L. P. Pitaevskii, *Electrodynamics of Continuous Media* (Elsevier, New York, 1984).
[13] K. Miyake and H. Kohno, J. Phys. Soc. Jpn. **74**, 254 (2005).
[14] G. D. Mahan, *Many-Particle Physics* (Plenum, New York, 1981).
[15] C. Grenzebach, F. B. Anders, G. Czycholl, and T. Pruschke, Phys. Rev. B **74**, 195119 (2006).
[16] V. Zlatić and R. Monnier, Phys. Rev. B **71**, 165109 (2005).
[17] P. Link, D. Jaccard, and P. Lejay, Physica B **225**, 207 (1996).
[18] A. L. Cornelius, J. M. Lawrence, J. L. Sarrao, Z. Fisk, M. F. Hundley, G. H. Kwei, J. D. Thompson, C. H. Booth, and F. Bridges, Phys. Rev. B **56**, 7993 (1997).
[19] J. L. Sarrao, C. D. Immer, C. L. Benton, Z. Fisk, J. M. Lawrence, D. Mandrus, and J. D. Thompson, Phys. Rev. B **54**, 12207 (1996).
[20] H. B. Callen, Phys. Rev. **73**, 1349 (1949).
[21] J. M. Luttinger, Phys. Rev. **135**, A1505 (1964).
[22] C. A. Domenicali, Rev. Mod. Phys. **26**, 237 (1954).
[23] T. Costi, A. Hewson, and V. Zlatić, J. Phys.: Condens. Matter **6**, 2519 (1994).
[24] R. D. Barnard, *Thermoelectricity in Metals and Alloys* (Taylor & Francis, London, 1972).
[25] G. D. Mahan, in *Solid State Physics* (Academic, San Diego, 1998), Vol. 51, p. 81.
[26] A. Khurana, Phys. Rev. Lett. **64**, 1990 (1990).
[27] J. K. Freericks and V. Zlatić, Rev. Mod. Phys. **75**, 1333 (2003).
[28] J. K. Freericks and V. Zlatić, Phys. Rev. B **64**, 245118 (2001).
[29] W. Metzner and D. Vollhardt, Phys. Rev. Lett. **62**, 324 (1989).
[30] U. Brandt and C. Mielsch, Z. Phys. B: Condens. Matter **75**, 365 (1989).
[31] A. Georges, G. Kotliar, W. Krauth, and M. J. Rozenberg, Rev. Mod. Phys. **68**, 13 (1996).
[32] A. C. Hewson, *The Kondo Problem to Heavy Fermions* (Cambridge University Press, Cambridge, 1993).
[33] K. Yamada and K. Yosida, Prog. Theor. Phys. **76**, 621 (1986).
[34] K. Yamada, *Electron Correlation in Metals* (Cambridge University Press, Cambridge, 2004).
[35] N. S. Vidhyadhiraja and D. E. Logan, Eur. Phys. J. B **39**, 313 (2004).
[36] D E Logan and N S Vidhyadhiraja, J. Phys.: Condens. Matter **17**, 2935 (2005).
[37] A. Hübsch and K. W. Becker, Eur. Phys. J. B **52**, 345 (2006).
[38] M. Kim, Y. Nakai, H. Tou, M. Sera, F. Iga, T. Takabatake, and S. Kunii, J. Phys. Soc. Jpn. **75**, 064704 (2006).
[39] S. Kobayashi, Y. Yoshino, S. Tsuji, M. Sera, and F. Iga, J. Phys. Soc. Jpn. **72**, 25 (2003).
[40] In Kondo systems with small T_K, the paramagnetic entropy is removed at $T_c > T_K$ by a magnetic phase transition. In such systems the low-temperature maximum of $\alpha(T)$ might be concealed and it will emerge only if the FL state is restored by pressure or magnetic field, but these additional complications are neglected here.
[41] N. E. Bickers, D. L. Cox, and J. W. Wilkins, Phys. Rev. B **36**, 2036 (1987); N. E. Bickers, Rev. Mod. Phys. **59**, 845 (1987).
[42] V. Zlatić, R. Monnier, and J. Freericks, Physica B **380-382**, 661 (2006).
[43] K. Hanzawa, K. Yamada, and K. Yosida, J. Magn. Magn. Mater. **47&48**, 357 (1985).
[44] J. K. Freericks and V. Zlatić, Phys. Rev. B **58**, 322 (1998).
[45] J. K. Freericks, D. O. Demchenko, A. V. Joura, and V. Zlatić, Phys. Rev. B **68**, 195120 (2003).
[46] A. V. Joura, D. O. Demchenko, and J. K. Freericks, Phys. Rev. B

69, 165105 (2004).
[47] N. Kernavanois, S. Raymond, E. Ressouche, B. Grenier, J. Flouquet, and P. Lejay, Phys. Rev. B **71**, 064404 (2005).
[48] D. Gignoux and J. C. Gomez-Sal, Phys. Rev. B **30**, 3967 (1984).
[49] V. Zlatić and J. Freericks, Acta Phys. Pol. B **34**, 931 (2003).
[50] C. Dallera, M. Grioni, A. Shukla, G. Vankó, J. L. Sarrao, J. P. Rueff, and D. L. Cox, Phys. Rev. Lett. **88**, 196403 (2002).
[51] D. Withoff and E. Fradkin, Phys. Rev. Lett. **64**, 1835 (1990).
[52] S. Burdin and V. Zlatić, arXiv:cond-mat/0212222 (unpublished).
[53] J. N. Hancock, T. McKnew, Z. Schlesinger, J. L. Sarrao, and Z. Fisk, Phys. Rev. Lett. **92**, 186405 (2004); Phys. Rev. B **73**, 125119 (2006).
[54] J. L. Sarrao, Physica B **259&261**, 261 (1999).
[55] M. Očko, C. Geibel, and F. Steglich, Phys. Rev. B **64**, 195107 (2001).
[56] M. Očko, D. Drobac, B. Buschinger, C. Geibel, and F. Steglich, Phys. Rev. B **64**, 195106 (2001).
[57] M. Očko, J. L. Sarrao, I. Aviani, Dj. Drobac, I. Živković, and M. Prester, Phys. Rev. B **68**, 075102 (2003).